FINAL PUBLISHABLE JRP REPORT

JRP-Contract number	NEW07
JRP short name	THz Security
JRP full title	Microwave and terahertz metrology for homeland security
Version numbers of latest contracted Annex Ia and Annex Ib against which the assessment will be made	Annex Ia: V1.2 Annex Ib: V1.2
Period covered (dates)	From 01 June 2012 To 31 May 2015
JRP-Coordinator	
Name, title, organisation	Dr. Thomas Kleine-Ostmann, Physikalisch-Technische Bundesanstalt (PTB)
Tel:	+49-531-592-2210
Email:	thomas.kleine-ostmann@ptb.de
JRP website address	http://www.ptb.de/emrp/thz_security.html
Other JRP-Partners	
Short name, country	CMI, Czech Republic INRIM, Italy LNE, France SFI Davos, Switzerland SMU, Slovakia R&S, Germany SLT, Germany

REG1-Researcher (associated Home Organisation):	Sven Augustin TUB, Germany	Start date: 01 January 2013 Duration: 12 months
REG2-Researcher (associated Home Organisation):	Gunter Urbasch UMR, Germany	Start date: 01 August 2012 Duration: 18 months
REG3-Researcher (associated Home Organisation):	Juliette Mangeney CNRS LPA, France	Start date: 01 December 2012 Duration: 20 months

Report Status: PU Public

REG4-Researcher (associated Home Organisation):	Gunter Urbasch UMR, Germany	Start date: 01 February 2014 Duration: 16 months
RMG1-Researcher (associated Empl. Organisation)	Martin Hudlička CMI, Czech Republic (guestworking at PTB)	Start date: 01 March 2013 Duration: 9 months
RMG2-Researcher (associated Empl. Organisation):	David Jahn UMR, Germany (guestworking at INRIM)	Start date: 01 October 2013 Duration: 13 months
RMG3-Researcher (associated Empl. Organisation):	Sina Lippert UMR, Germany (guestworking at INRIM)	Start date: 01 November 2013 Duration: 4 months

TABLE OF CONTENTS

1   Executive Summary

Microwave (millimetre) and terahertz (THz) (sub-millimetre) detection devices have great potential for use in homeland security. But the development and use of these devices was being held back as important performance properties could not be measured reliably – limiting their effectiveness, and preventing an accurate assessment of the effects of exposure to the radiation they emit. This project developed methods to calibrate microwave and terahertz instrumentation against SI unit definitions, and validated an approach to assess the effects of the radiation. The techniques are being used to develop the next generation of security scanners, offering dramatically improved, fast, safe and non-invasive scanning.

The Problem

Microwave and terahertz radiation have the potential to transform defence and homeland security, offering better detection and increased security, coupled with faster and more comfortable security checks. Personal scanning devices operating at these wavelengths can quickly and non-invasively image through clothing to identify concealed weapons, drugs and other contraband items, whilst THz spectrometers can analyse substances such as liquids in real-time to determine their composition.

Microwave scanning technology is already in development, and the first commercial scanners are currently being trialled in airports worldwide. The use of higher-performance THz scanners and spectrometers has been demonstrated in the laboratory, and they represent the future of security scanning devices. However, the development and use of microwave and THz detection was hampered by a lack of certainty in their performance. Different devices reported varying results in identical tests, and measurements could not be traced back to the SI unit definitions, so levels of accuracy and uncertainty could not be determined reliably. Techniques were needed to calibrate important performance parameters against SI definitions, such as frequency, amplitude and power. And, to satisfy existing and future safety requirements, methods were needed for assessing the effects of exposure to microwave and THz radiation for people being scanned, and for people operating the devices.

The Solution

This project has developed measurement capabilities to support the development of reliable and accurate microwave and THz detection devices. A suite of complementary techniques to calibrate microwave and THz detectors was designed, and then used to develop specific techniques to calibrate THz spectrometers. These techniques were then used to compare the performance of THz spectrometers and to accurately determine measurement uncertainty. Finally, modelling approaches were validated for assessing the effects of exposure to the microwave and THz radiation.

Impact

This project has substantially improved microwave and THz measurement accuracy and reliability, making these technologies readily accessible for security applications. The project initiated first standardisation activities for spectrometers and scanners in the millimeter wave and THz region of the electromagnetic spectrum, and, thus, is paving the way for reliable measurements in this wavelength range.

The project allows quantification of the human exposure to (sub-)mm waves to monitor the compliance with safety limits and provide data for further regulatory action in the future. Results may contribute to two overarching standards, IEC/EN 62479 and IEC/EN 62311, which govern the protection of people exposed to electromagnetic fields when using novel devices for which product standards have not yet been established. These standards are a prerequisite for new hardware development, and are essential for securing the public acceptance of new technologies that use electromagnetic radiation. The techniques developed during this project will also be used to demonstrate compliance with European Directive 2004/40/EC "Physical Agents Directive", which sets exposure limits for personnel working with high-frequency radiation, as well as for other applicable national and international guidelines.

For the first time, a range of methods are now available for industrial users and research laboratories to calibrate THz instruments against measurement unit definitions. The THz detector calibration service offered by PTB was used more than 20 times by the end of the project, by manufacturers and research institutions from China, Japan, USA, Russia, France and Germany. The new pyro-electric detectors, to be used as calibration transfer standards, can be purchased from SLT GmbH. The room-temperature radiometer developed at SFI Davos is available for customers, such as small research laboratories, to establish traceability to measurement definitions outside of the calibration service.

2   Project context, rationale and objectives

The need to improve homeland security, for example by establishing person scanning and the identification of suspicious substances at airports, has led to the development of new security systems based on microwave (millimetre) and THz (sub-millimetre) technology. Microwave scanning technology is already in development, and the first commercial scanners are currently being trialled in airports worldwide. The use of higher-performance THz scanners and spectrometers has been demonstrated in the laboratory, and they represent the future of security scanning devices. Personal scanning devices operating at these wavelengths can quickly and non-invasively image through clothing to identify concealed weapons, explosives, drugs and other contraband items, whilst THz spectrometers can analyse substances in real-time to determine their composition, such as analysing liquids to identify the presence of explosives, drugs, or chemical or biological weapons. These technologies offer the potential of better detection and increased security, coupled with faster and more comfortable security checks.

However, the development and use of microwave and THz detection systems has been hampered by a lack of certainty in their performance. Different devices reported varying results in identical tests, and measurements could not be traced back to the SI unit definitions, so levels of accuracy and uncertainty could not be determined reliably. Techniques were needed to calibrate important performance parameters against SI definitions, such as frequency, amplitude and power. And, to satisfy existing and future safety requirements, methods were needed for assessing the effects of exposure to microwave and THz radiation for people being scanned, and for people operating the devices.

These will be the prerequisites for future standardisation activities for personnel scanners and THz spectrometers within the International Electrotechnical Commission (IEC) or CENELEC (Comité Européen de Normalisation Électrotechnique).

Activities for the standardisation of X-ray security scanners have started recently, and resulted in the new standard DIN IEC 62463:2010. The use of new millimetre and THz technology requires conformity with the safety limits for electromagnetic field exposition that exist up to 300 GHz. Based on the guidelines of the International Commission on Non-Ionizing Radiation Protection (ICNIRP), the European Directive EC 2004/40/EC "Physical Agents Directive" sets limits for working personnel between 2 GHz and 300 GHz (50 W/m^2 in controlled environments). Before this project, no reliable measurement capabilities existed to assess the human exposure for scanned persons and operating personnel using millimetre and THz systems. Traceability to SI units, with uncertainties less than 20%, currently lacking, are similarly crucial for authorities in the approval of the use of scanners for the public.

Certain materials in the security sector exhibit characteristic spectral features in the terahertz region allowing for specific identification of a particular compound. THz radiation is able to propagate through non-conducting and non-polar material (i.e. clothing, plastics, paper and cardboard) which can reveal security threats through various packaging. The THz technology showcases its potential uses in the security industry as it can also use the same system to detect drugs of abuse and other illegal materials. Exact and traceable verification of the frequency and amplitude of the spectra is necessary in order to distinguish correctly among various explosives, drugs and other illicit materials with unique spectral fingerprints. Passive THz imaging is an exposure-free alternative which enables real-time imaging and detection of hidden objects. The quality of passive imaging relies strongly on efficient use of the bandwidth between 200 GHz and 1 THz. There is a strong need for accurate and reliable characterisation capabilities of frequency and power responses of the detectors and the optics as well as material properties in this range to quantify the possibilities and the limitations of passive imaging.

The properties of microwave and THz radiation being non-ionising and penetrating through most cloth materials have led to the development of personnel scanners. Active scanners illuminate a scanned object or person with electromagnetic waves and detect the reflected radiation, while passive scanners measure the radiation emitted or reflected by a person or object. While the personnel scanners tested at airports right now operate at frequencies between 20 GHz and 100 GHz, active remote scanning has also been demonstrated at higher frequencies and might be used in the next generation of scanners. Passive scanners work at the frequency range of 200 GHz – 1 THz. While current scanner technologies are pure imaging systems, spectral information might be used in the future that improves the capability of such systems to distinguish between dangerous and harmless materials (e.g. between explosives and plastics) worn on the body and also distinguish these materials from non-threat materials such as clothing that a person may be carrying. Ultra-wideband radar systems might be used for through-wall people detection and might be capable of measuring human heart and breathing rates from a distance, for security purposes. With THz time-domain spectroscopy, the detection of various illegal and dangerous substances such as drugs, explosives, poisons

and biological weapons has been demonstrated based on the spectral fingerprints of these substances. However the systems have to be further improved to identify the substances unambiguously (accuracy and dynamic range in order to avoid influence of the spectra of barrier materials, scattering from rough surfaces etc.). THz spectrometers could contribute to the security check on airports or other security relevant locations where other security technologies do not provide acceptable solutions, e.g. for the fast identification of liquids. Active THz imaging, whether using spectral information or not, can be used for various security applications, e.g. for mail inspection, inspection of bags or for remote sensing in dangerous scenarios. However, measurement data produced by different spectrometers often differ significantly regarding the amplitude and frequency (often by several 10 %) of spectral features. The necessary metrology to determine the properties of scanners and spectrometers as needed for the evaluation of benefit, the improvement of technology and the assessment of possible adverse health effects does not exist so far. Even the leading metrology institutes in this area outside Europe such as NIST and NMIJ/NICT do not provide traceability in the frequency range of interest up to 5 THz. Traceable field probe calibration is only available up to 40 GHz so far. However, above 20 GHz practical measurements using such field probes have limited value if the field geometry is unknown. Radio frequency power measurements with high accuracy below 1 % are only available in coaxial lines and the lower waveguide bands below 110 GHz, but not for radiated waves. Traceability of radiation power as needed to determine radiation power densities and field strengths has only been established for collimated beams based on detector radiometry at a single selected frequency of 2.52 THz. Here, a standard uncertainty in the order of 10 % could be achieved. For diffuse radiation, calculable blackbody sources have been used to calibrate more sensitive detectors with much larger standard uncertainties. However, no procedures exist to transfer the calibration to pulsed spectrometers or to scanners using complex antenna and frequency diversity schemes. Measurements on personnel scanners have been performed in the course of authorisation decisions for field tests without a scientific basis of how to evaluate average and peak values. Only very preliminary attempts to model the uncertainty of different kinds of THz spectrometers have been undertaken so far. Exact approaches to calibrate the frequency axis of spectrometers, e.g. based on frequency combs that could be used to measure the absolute frequency of tunable THz sources, do not exist throughout the whole THz frequency range at present.

Four objectives were identified to achieve the overall goal of developing measurement capabilities to support the development of reliable and accurate microwave and THz detection devices. Objective 1 developed a suite of complementary techniques to calibrate microwave and THz detectors. Objective 2 used the results of objective 1 to develop specific techniques to calibrate THz spectrometers. These techniques were then used in objective 3 to compare the performance of THz spectrometers and to accurately determine measurement uncertainty. Objective 4 validated modelling approaches for assessing the effects of exposure to the microwave and THz radiation.

1. To extend existing capabilities for characterisation and calibration of sources and detectors, traceable to the SI units, from the existing single frequency capability of 2.52 THz, to a wide frequency range from 20 GHz to 5 THz. This includes both the extension of calibration facilities at National Metrology Institutes, as well as the development of new detectors suitable for transfer and dissemination of the calibration to customers from science, industry and regulation authorities.

2. To establish traceability of amplitude, phase and frequency for pulsed time-domain, vector network analysis (VNA) based and Fourier-Transform Infrared (FTIR) spectrometers and to develop reference materials for spectrometer validation. This is the basis for the evaluation of the measurement uncertainty of THz spectrometers.

3. To assess the performance of pulsed time-domain, VNA-based and FTIR spectrometers, by comparison of their uncertainty. This results in an evaluation of the measurement uncertainty which is a prerequisite for meaningful results.

4. To assess the radiated power flux densities of different types of microwave and THz scanners, and to use the results for realistic dosimetry, by development of numerical skin models and phantoms, as a basis both for performance and safety evaluation of such systems. This will enable regulation authorities to base their evaluation concerning the harmfulness of THz radiation on validated facts.

3 Research results

In this section the research results of the four main scientific objectives will be described.

3.1 Extension of capabilities for characterisation and calibration of sources and detectors, traceable to the SI units

The objective of this work was to establish traceability for sources and detectors of THz radiation over a wide frequency range from 20 GHz to 5 THz as needed to close the measurement chain from applied measurement systems such as scanners and spectrometers to the representation of the SI units. This includes characterisation of beam properties as well as the development of calibration procedures for a wide range of detectors for different categories of THz radiation depending on signal shape (pulsed or continuous wave), frequency range and power. It also includes the development of means for the practical transfer of amplitude calibration to THz systems.

Detector Calibration and Measurements

Up to now, the calibration of spectral responsivity of THz detectors by means of laser radiation was possible only at 2.52 THz. Beside these services offered exclusively by PTB there are no other THz standards worldwide. A core instrument of PTB's THz detector calibration facility is a THz molecular gas laser optically pumped by an integrated single-frequency CO_2-laser. Its tuning range from 1 THz to beyond 5 THz is based on discrete THz lines in different gases, such as e.g. CH_3OH, CD_3OH, CH_2F_2.

This THz laser with output power in the mW range and well examined beam quality was be used to establish traceability at its other molecular gas lines above and below 2.52 THz. The expansion to its full tuning range from 1 THz to beyond 5 THz requires a reference detector that is carefully characterised to understand its THz radiation absorption. The reference detector is a commercially available but modified thermopile detector using a volume absorber for the radiation detection. The wavelength depending reflection of the surface and the transmission of the absorber had to be measured. The real power at a given frequency is then the sum of the measured power and the known, well characterised radiation losses. These losses can be measured quantitatively by comparison with the standard detector at 2.52 THz, but must be derived from physical principles and further measurements at other frequencies.

Fig. 3.1.1: PTB's new "gold standard" for detector-based THz radiometry: The cutaway view exhibits a schematic cross-section of the THz radiation absorber with gold (Au) coating on its back side. Part of the incoming (1) radiation is reflected (2) at the front side. The lack of interference modu¬lation of this radiation indicates no remarkable residual (3) radiation after two passes through the absorbing disc enabled by the gold coating.

First performed at 2.52 THz only, PTB has now extended its unique detector-based radiometric calibration service to the full tuning range of a THz laser spanning from 1 THz to 5 THz. As published in Optics Express (Andreas Steiger et al., 2013), the standard measurement uncertainty of the THz power scale is reduced simultaneously to below 2 % by a new way to link the scale to the International System of Units (SI).

In detail, an optically polished neutral density glass disc is coated with a thin gold layer on the back side and mounted as a special broad band THz radiation absorber inside a commercial laser power meter as shown in Fig. 3.1.1. In the case of incomplete absorption during the first pass through the disc, the remaining radiation is reflected by the gold mirror to experience a second absorption process. By this, the radiation loss is dominated by the front surface reflection. Moreover, the reflected radiation has been measured precisely at all spectral emission lines of a THz molecular gas laser and in the visible spectrum as well. As a consequence, the power responsivity of such a modified laser power meter can be determined with the lowest possible uncertainty by means of a HeNe laser in the visible and extrapolated into the THz regime.

Hence the question "How much THz power do I have?" is solved because reliable THz power measurements with known accuracy are possible now. As of late, the traceable calibration of suitable THz detectors in the wide spectral range from 1 THz up to 5 THz has become part of the official services of PTB offered world-wide to customers in research and industry.

The first international comparison of THz laser power measurements took recently place at PTB in Berlin. Andreas Steiger hosted the comparison with the visiting scientists Yuqiang Deng and Qing Sun from the National Institute of Metrology (NIM) of China and John Lehman of the National Institute of Standards and Technology (NIST) who is presently visiting PTB as a Research Fellow of the Alexander von Humboldt Foundation of Germany. Measurements were carried out at two frequencies, 2.52 THz and 762 GHz and at a power level of approximately 3 mW. The measurement results from each participant agreed very well with the reference value and to each other within the stated uncertainties.

This pilot comparison was undertaken in a relatively short period from May 4th to 8th, 2015. Typically, such key comparisons may last years. Organised in a new manner, the participants met in Berlin to compare their standards at one place at one time. The measurement infrastructure such as the laser source and other instrumentation provided by PTB were critical to meeting the proposed schedule.

Three different national THz standard detectors were used for the comparison of their spectral power responsivity. The PTB standard for 762 GHz is a thin-film pyroelectric THz detector as shown in Fig. 3.1.2 which has been developed in cooperation with Sensor- und Lasertechnik (SLT). It consists of a 12 µm thin pyroelectric polyvinylidene fluoride (PVDF) foil coated on both sides with a thin layer of a metal oxide. These layers are conductive and serve two objectives: each layer is one electrode to catch the charge generated by the pyroelectric effect of the foil when the temperature changes; both layers, together, compose the absorber for the THz radiation. The sheet resistance of both layers is carefully adjusted via their combined thicknesses to match half the vacuum impedance. In this case 50% of the power is absorbed in the metal oxide layers whereas 25% of the power is reflected and 25% transmitted. The transmitted radiation is absorbed inside the detector housing. Following Maxwell´s theory and verified by THz-TDS measurements this absorbance is frequency independent in a wide spectral range from the low GHz range to several THz. Therefore this thin-film pyroelectric detector could be calibrated at a frequency of 1.04 THz and also at 1.40 THz by comparison with PTB's reference detector using the continuous-wave THz laser at the THz calibration facility.

The comparison was performed according to the guidelines provided by the Consultative Committee on Photometry and Radiometry (CCPR). The results have still to be approved by the CCPR and will then be published for a larger community. The work represents the first key comparison ever undertaken in the far-infrared spectral region. It represents a milestone which will greatly benefit commercial development of instrumentation and sensors for remote sensing, THz imaging, high-speed telecommunications and time-domain spectroscopy.
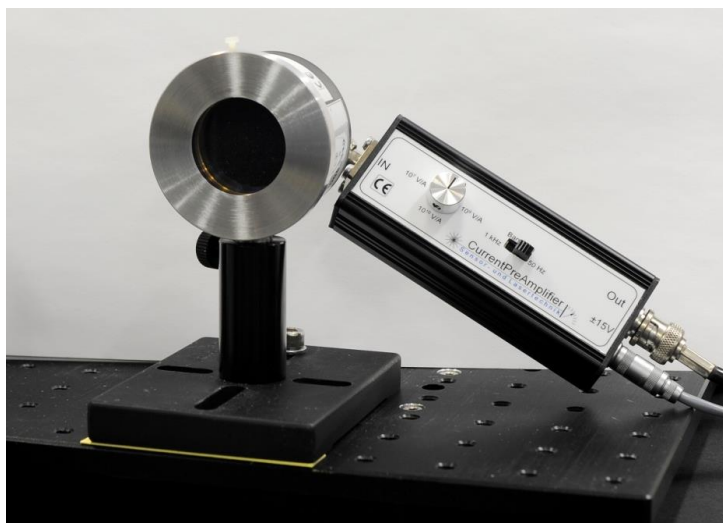
Fig. 3.1.2: Photograph of the thin-film pyroelectric detector. The current amplifier is seen to the right.

For practical applications, traceable measurements have to be performed at other frequencies in the microwave and sub-THz region, also. Since classical field standards based on traceable measurements of radio frequency power and antenna gain are available up to 40 GHz only, the remaining gap to 1 THz had to be closed. Here, a large area detector based on a gas cell can be applied. It measures the thermal extension due to radiant heating with an acoustic detector. The existing detector allows a traceable measurement of the radiant power in a collimated Gaussian beam incident under the Brewster angle by direct substitution with electrical heating power. In order to set up a reliable measurement uncertainty budget, extensive studies on the properties of the detector including transmission properties of the window, homogeneity of the detector area, long- and short-term stability and environmental parameter dependence had to be performed. The detector was applied to measure the radiant power densities of different sources used throughout the project. The results had to be compared systematically in order to evaluate the performance of the different methods. After that the large area detector was used to transfer the radiant power to arbitrary sources with frequencies between 20 GHz and 5 THz and it was used to measure the irradiance.

Most applications of mm- and sub-mm waves use collimated Gaussian beams to direct the THz wave to the object under test or the human being that is scanned. Examples are security scanners, spectrometers or systems for the quality control of industrial products but also ranging and communication systems. All these systems have in common that THz optics such as parabolic or elliptic mirrors or dielectric lenses are used for THz beam shaping. In many applications, e.g. in spectrometers, the THz wave has to be focused onto a sample in order to increase the interaction between THz wave and matter and in almost all applications the THz wave needs to be focused onto a detector in order to gain sensitivity.

In many of these systems, the accurate knowledge of the beam properties (e.g., beam profile and power density) with less than 1 % uncertainty is crucial. Using a THz source as local oscillator in a heterodyne system (e.g. in radio astronomy or atmospheric sensing) requires accurate beam quality and hence very sophisticated THz optics that cannot be optimised without the ability to measure the beam profile. Another example where the beam property is crucial is the dosimetry for field exposure with THz radiation. Reliable and significant experiments to determine possible detrimental effects of THz radiation on biological samples require the accurate knowledge of the power flux density with uncertainties of a few percent or less at the location of the sample. Only with the knowledge of the spatial distribution of the exposure fields the specific absorption rate (SAR) which is a measure for the exposition strength, can be determined quantitatively.

Up to now the capability to determine the beam profile accurately was rather limited. Only at higher frequencies of at least a few hundred GHz pyro-electric cameras can be used to measure beam profiles. However, no uncertainty assessment was performed so far. At lower frequencies no such measurements could be performed due to lacking sensitivity and detector size and THz optics in this frequency range are far from optimum since their design has been based on assumptions, only. At frequencies below 500 GHz also the traditional knife edge method, which is extensively used in optics to measure beam profiles, fails. Here, a sharp edge is moved through the beam. The derivative of the power measurement yields the beam profile.

For mm-wave this method fails due to standing wave and diffraction between the sharp edge, lens and power detector.

Recently, a new method was proposed to measure beam profiles at low frequencies using the tip of a dielectric fibre coupled to a power meter. The tip can be used to perform a two-dimensional scan of the beam profile without disturbing the original field too much. For this objective the capabilities of this method was examined extensively and it was extended to a large frequency range between 20 GHz and 500 GHz. As an alternative method, bolometer elements were used to perform beam measurements. The advantages of both methods were compared. At higher frequencies, a pyro-electric camera was applied for beam scans. New approaches for a pixel based calibration of these cameras were implemented. For all sources used within this Joint Research Project, the most suitable method was applied to characterise the beams. Beam characterisation within this project was required for the sources used in detector radiometry (e.g. far-infrared lasers and quantum cascade lasers) but also for the uncertainty analysis of the vector-network analysis based spectrometers and the exposition assessment of the personnel scanners.

Development of a portable room-temperature radiometer

The radiometer shown in Fig. 3.1.3 and 3.1.4 is based on the principle of electrical substitution of the radiation absorbed in an absorbing cavity, similar to what is currently being used as primary reference for solar irradiance measurements and in optical laboratories.

Fig. 3.1.3: The new PMO-THz radiometer (right side) together with the modified thermopile PTB THz-Standard-Detector.
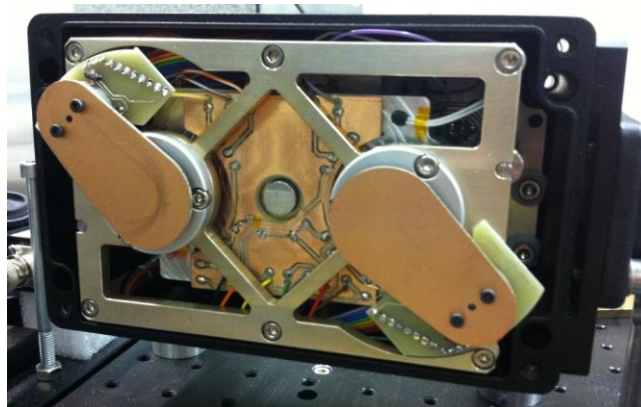

Fig. 3.1.4: Interior of the PMO-THz electrical substitution radiometer. Both cavities, here covered by their individual shutter blade, can be used as active cavities for THz power measurements.
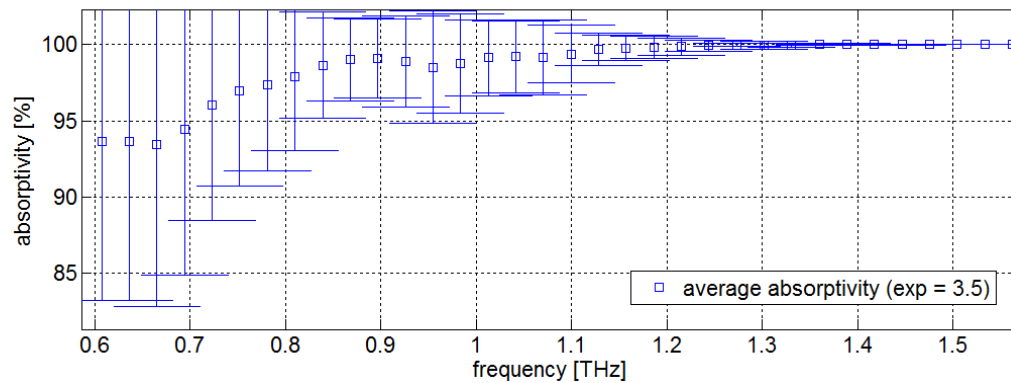
Fig. 3.1.5: Absorptivities of the cone shaped PMO-THz radiometer cavities including their uncertainty. For frequencies f > 1.5 THz, the absorptivity of the cavity becomes > 99.99 % and therefore the uncertainty of the radiometer decreases to less than 500 ppm.

The total absorbance was maximised by making use of multiple absorption in a properly designed cavity. As can be seen in Fig. 3.1.5, we encountered a lower total absorbance than what is achievable in the visible light spectrum, where cavities absorb up to 99.99 % of the incoming radiation, at lower frequencies, only. The cavity geometry was optimised to equalise the spatial heat dissipation within the cavity in the radiated and shaded states, respectively. This minimises the non-equivalence of electrical and radiative heating and hence guarantees the accurate electrical substitution.

Fig. 3.1.6 shows a comparison between power measurements using the new radiometer and the PTB standard detector at four different frequencies. The discrepancies between the two detectors obtained for $f = 1.40$ THz indicates that the absorptivity for THz detectors at different THz frequencies is not yet sufficiently understood. Further detailed investigations of wavelength dependent THz radiation absorptivities are necessary to resolve this disagreement, leading to more accurate power measurements of THz radiation in future.
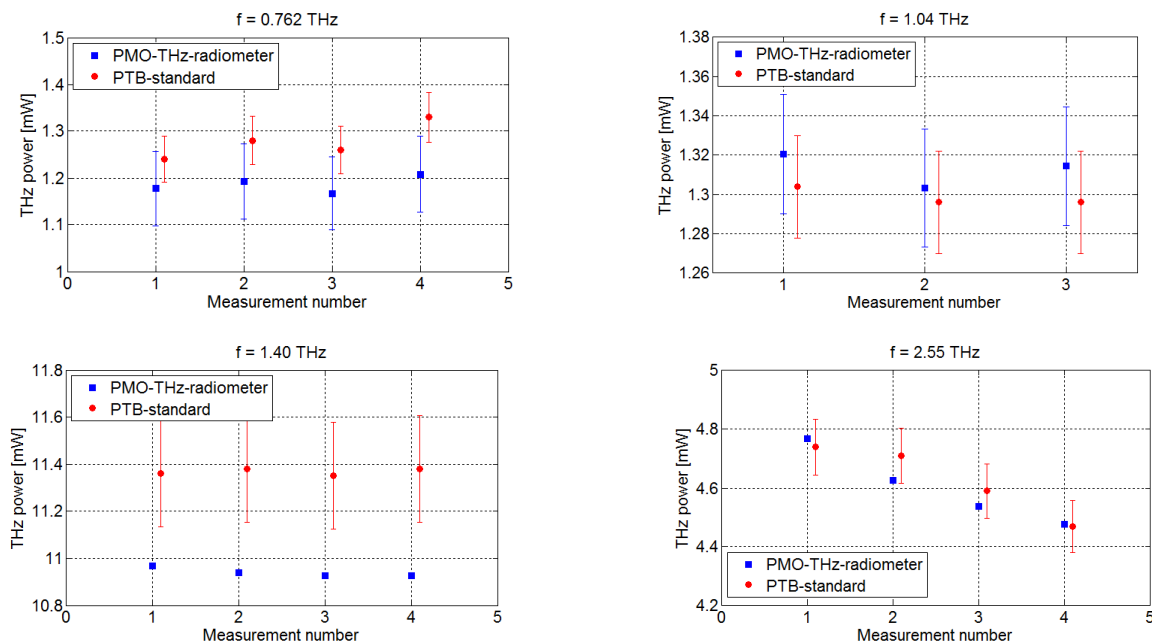

Fig. 3.1.6: The power measurements with the PMO-THz radiometer generally agree well with the PTB standard detector results within their stated measurement uncertainties. Except for f = 1.40 THz, the PMO-THz radiometer measured about 3.8 % lower power values than the PTB standard. For f = 0.762 THz, a pyroelectric thin-film THz detector is used as the PTB standard instead of the modified thermopile detector.

Microbolometers

The microbolometer to be developed and fabricated at SMU, is based on $LaSrMnO_3$ thin film disc placed in the feed point of logarithmically periodic thin-film antenna, both of them deposited on GaN MEMS structure ensuring efficient thermal isolation. JRP-Partners from SMU visited PTB in Berlin to perform calibration of the microbolometer response to radiant power exploiting the calibration facility at PTB. Another task was to determine partial uncertainties and make an uncertainty budget of the calibration. The microbolometer was used as an alternative method for beam profile analysis. The single microbolometer was designed in such a way to allow for its future integration into a line of microbolometers being suitable for applications in security imaging.

The microbolometer was tested in PTB Berlin (Dr. Steiger) at two frequencies 1.4 THz and 0.762 THz. In both cases the diameter of the laser beam was about 2 mm and its power 1.615 mW. The results of the beam scanning are shown Fig. 3.1.7 and Fig. 3.1.8.
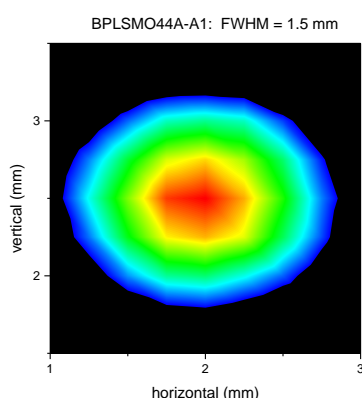

Fig. 3.1.7: Two-dimensional power density diagram of a laser beam of the frequency of 1.4 THz. Reference sensor power (the same optical path as a microbolometer) was 1.615mW. Sensor bias current I_{dc} = 100uA, voltage drop across its terminals dV=71.7 mV, V_{ac} = 42uV.
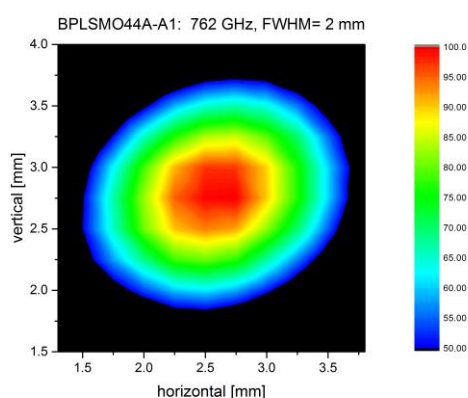
Fig. 3.1.8: Power density diagram of a laser beam f= 762 GHz.

Besides this, we have also measured the polarisation diagram (Fig. 3.1.9). The diagram shows that the antenna increases the sensitivity of the microbolometer about 4 times compared to bare LSMO disc (when the polarised radiation impacts perpendicularly to the antenna axis).
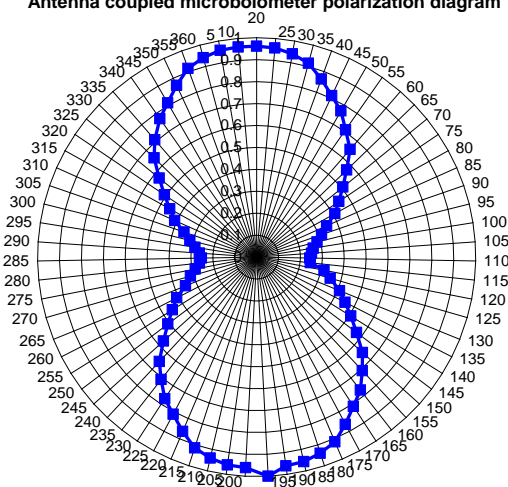

Fig. 3.1.9: Polarisation diagram of the micro-bolometer with log-periodic antenna.

The microbolometer was fabricated using MEMS technology known from microelectronics. The core element is a bolometric disc made of advanced material $La_{0.67} Sr_{0.33} MnO_3$ that exhibits very steep R(T) dependence as shown below in Fig. 3.1.10 (red curve). The derivative of R(T) (green curve) shows that the optimal operating temperature is about 65 °C at which the microbolometer sensitivity is the highest (corresponding temperature coefficient of resistance *TCR* = 0.017 K^{-1} which is about 5 times higher value than that of metals). It implies that the task to fabricate uncooled microbolometer has been accomplished.
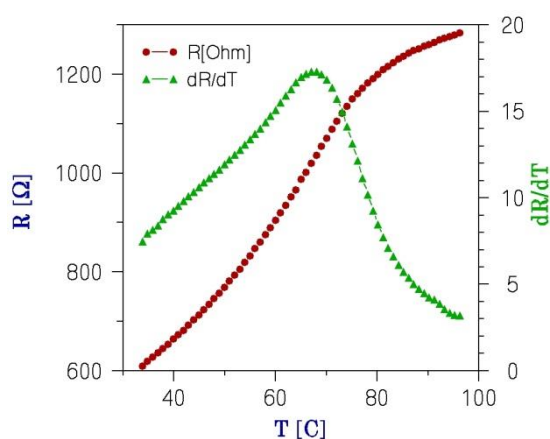

Fig. 3.1.10: Temperature dependence of resistance of bolometric LSMO film. Its derivative shows that the optimal operating temperature is 65 °C. It means the microbolometer is not only uncooled – it must be heated above room temperature, which is advantageous for stabilisation of the temperature setpoint.

The schematic drawing of the microbolometer is shown in Fig. 3.1.11 and the close-up photograph of the real microbolometer chip in Fig. 3.1.12. As already mentioned, the microbolometer consists of LSMO disc placed in the feedpoint of thin-film log-periodic antenna made of gold. Both elements are placed on a 3 um thick silicon\silicon dioxide membrane in order to achieve good thermal isolation. The membrane was fabricated by deep reactive ion etching process (DRIE) applied from the bottom of SOI (silicon on insulator) substrate.
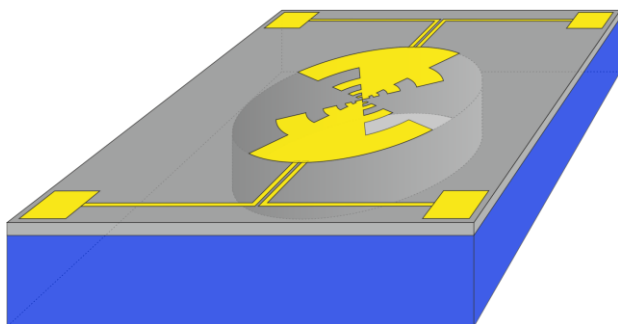

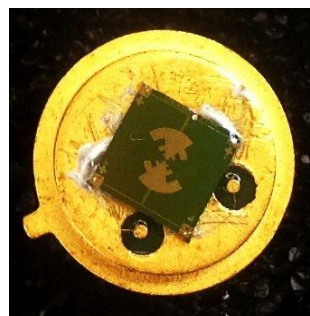Fig. 3.1.11: Schematic view of the microbolometer.

Fig. 3.1.12: Close-up photograph of the fabricated microbolometer. The holder is drilled below the membrane to avoid reflections of THz radiation from the bottom.

It is worth mentioning that the reproducibility of our technology is quite good – four microbolometers fabricated on the same SOI substrate had identical R(T) dependences.

Without a proper packaging of the microbolometer (a cap with THz window), it was not possible yet to calibrate it in a satisfactory way.

At the beginning of the project it was known from the literature that materials with perovskite structure (to which LSMO belongs) when irradiated by femtosecond laser pulse they can generate THz wave (Fig. 3.1.13). Our intention was to use this effect for on-chip testing or even calibration of the microbolometer. For

this task it was necessary to prepare high-resistivity LSMO film. Therefore, we prepared oxygen-deficient LSMOx film. The experiment on the structure shown in Fig. 3.1.14 was performed at TU Wien (Dr. Darmo). No emission of THz radiation was observed in THz time-domain spectroscopic setup. Meanwhile in the literature it was revealed that high resistivity is not the only condition to be fulfilled. The most suitable material is $PrCaMnO_3$ perovskite showing charge-ordering, this is presumably not the case in $LaSrMnO_{3-x}$ material. Further experiments are foreseen.
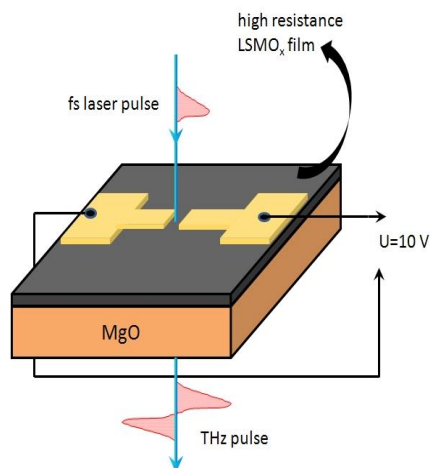
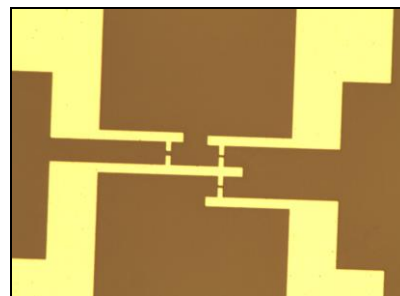Fig. 3.1.13: Principle of THz pulse generation by femtosecond laser pulse.

Fig. 3.1.14: Optical micrograph of three dipole antennae (gap size 5×10 μm^2 (twice), and 10×10 μm^2). The dipole length is 50 μm.

Summary

The objective to extend existing capabilities for characterisation and calibration of sources and detectors, traceable to the SI units, has been met to its full extent. The calibration facilities at National Metrology Institutes have been extended from the existing single frequency capability of 2.52 THz to a wide frequency range from 20 GHz to 5 THz. New detectors have been introduced including bolometers, pyroelectric detectors and a compact radiometer simplifying dissemination of the calibration to customers from science, industry and regulation authorities.

3.2 Establishment of traceability of amplitude, phase and frequency for THz spectrometers and development of reference materials for validation

This part of the project aimed to establish traceability for amplitude and frequency measurements of THz systems operating in the sub-THz and THz frequency range. In particular, existing scanning and spectroscopy systems like time-domain systems, VNA-based systems, and Fourier-Transform systems have been investigated quantitatively.

Traceability of time-domain THz systems

The aim of this task was to provide traceability for amplitude and frequency of THz systems. This was achieved using THz frequency combs. A rectification process has been used to transfer the optical frequency comb from a femtosecond laser to the THz frequency domain. Such a down-converted frequency comb can easily be utilised for the detection of continuous wave (cw) THz radiation to realise a detection method which benefits from the high measurement precision of an optical comb. The measurement process using a THz comb includes a heterodyne mixing process between one comb line and the cw-THz radiation. This results in a radio-frequency beating signal, which can be analyzed using standard electronics and which precisely reveals the frequency, amplitude, and phase of the signal to be determined.
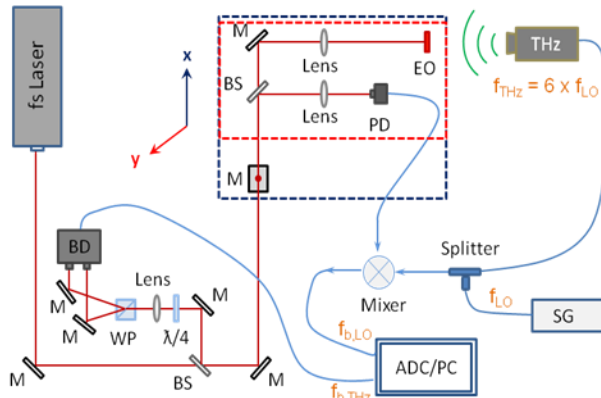
Fig. 3.2.1: Spatially resolved measurement setup: M: mirror, BS: beam splitter, EO: electro-optic crystal, PD: photodiode, SG: signal generator, ADC/PC: analog-to-digital converter and personal computer, WP: Wollaston prism, BD: balanced detector, λ/4: quarter-wave plate. The components comprised by the dashed red and blue rectangles can be moved in a direction parallel and perpendicular, respectively, to the optical table allowing for spatially resolved measurements.

The laser-based sampling setup developed at PTB is shown in Fig. 3.2.1. When the optical femtosecond pulses (which constitute an optical frequency comb) propagate through an electro-optic (EO) material, sidebands of the optical comb are generated by the THz field to be measured. The THz field was generated by a frequency multiplier chain set to a frequency of f_{THz} = 100.02 GHz. The sidebands are detected by guiding the femtosecond pulses that are back-reflected from the EO crystal to a typical EO detection setup. Here the beat $f_{b,THz} = |m\, f_{rep} \pm f_{THz}|$ with f_{rep}~76 MHz being the laser repetition rate is detected with a fast analogue-to-digital converter (ADC). This signal is proportional to the electric field of the THz source.

Due to the repetition rate fluctuation of the unstabilised laser, the THz beating signal drifts during the measurement interval and the recorded signal shows a spectral width of about 1-2 kHz. For high-precision measurements, this is usually avoided by stabilising the frequency comb.

We have followed a different approach to compensate for these fluctuations, based on a simple and versatile correction algorithm. In addition to the THz signal we simultaneously measure the fluctuations of the laser repetition rate. For this, the optical frequency comb is downconverted using a fast photodiode. Its output is mixed with a local oscillator set to f_{LO} and the mixing product $f_{b,rep} = |n\, f_{rep} \pm f_{LO}|$ is fed into the second channel of the ADC. A comparison between the two beating signals $f_{b,THz}$ and $f_{b,LO}$ allows us to reduce laser noise present in the amplitude measurements and also enables phase measurements of the THz source.

Now, the measured THz beating signal can be corrected for the laser repetition rate fluctuations using digital data processing. First, the frequency of $f_{b,rep}$ is multiplied by a factor m/n. Second, the resulting signal is mixed with the THz beating signal $f_{b,THz}$. After mixing the difference frequency is given by

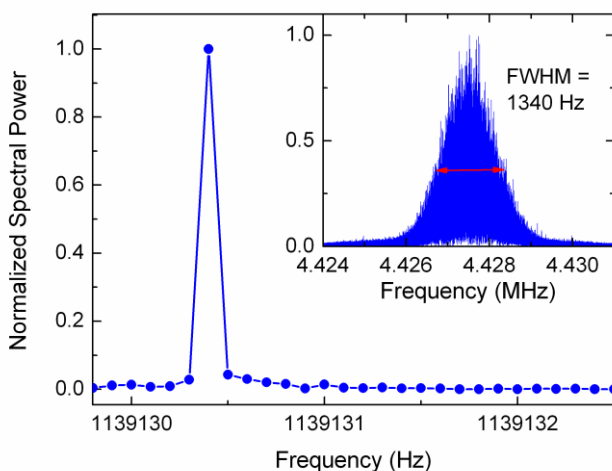$$f_{cor} = |m/n \cdot f_{LO} \pm f_{THz}|,\qquad(1)$$

Fig. 3.2.2: Normalized spectral power of the software-corrected THz beating signal. In the inset, the uncorrected measurement data is shown.

and, thus, does not depend on the repetition rate anymore. By applying the correction algorithm to the measured THz signal we obtain the corrected signal depicted in Fig. 3.2.2 with a resolution-limited FWHM of 0.1 Hz. Restating Eq. (1), f_{THz} can be obtained from the measured value for f_{cor}. The latter is extracted from the data using a software frequency counter. By this, we find a mean deviation of -0.009 Hz from the adjusted THz frequency, resulting in an accuracy as high as $9 \cdot 10^{-14}$ of the measurement setup.

The aforementioned setup can be enhanced for spatially resolved measurements. We have measured the spatially resolved intensity profile of a standard gain horn antenna at 107.6 GHz using the EO setup. Here a raster scanning technique over an area of 35 mm × 35 mm has been employed and the distance between the EO crystal and the horn antenna was 25 mm. We then measured the total power emitted from the antenna with a calibrated
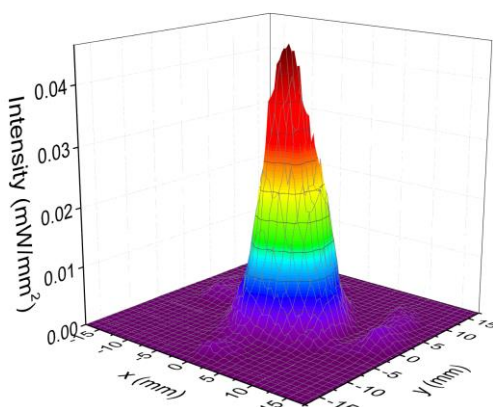
Fig. 3.2.3: Absolute intensity profile of the standard gain horn antenna at 100 GHz obtained from laser-based EO sampling.

THz radiometer and obtained a value of 3.32 mW. After some analysis including background subtraction, squaring of the spatially resolved EO signal, spatial integration, and comparison to the radiometer measurements, we obtain a normalisation constant for our laser based measurements. The resulting absolute, spatially resolved intensity distribution of the 100 GHz source is plotted in Fig. 3.2.3.

On the one hand, such measurements are important for the development of applications in this frequency range. On the other hand, the technique also helps to enlarge the frequency range of thermal radiometer measurements. It should also be mentioned that his technique is not only limited to the measurement of cw radiation but can also be applied to pulsed GHz and THz radiation.

Traceability of VNA-based THz systems

Measurement of intrinsic material properties such as the complex permittivity and permeability is very important in many scientific areas, e.g., microwave and millimeter-wave engineering (substrates, dielectric components), agriculture, material engineering and others. There exist different measurement techniques for different frequency bands and applications. Broadband free-space measurement techniques circumvent the problem of the precise fit of the sample to the measurement setup. A disadvantage is the need of a flat and homogeneous sample with relatively large dimensions to avoid diffraction effects. With the advance of measurement instrumentation, free-space systems for millimeter/sub-millimeter waves utilising vector network analyzers (VNA) became possible.
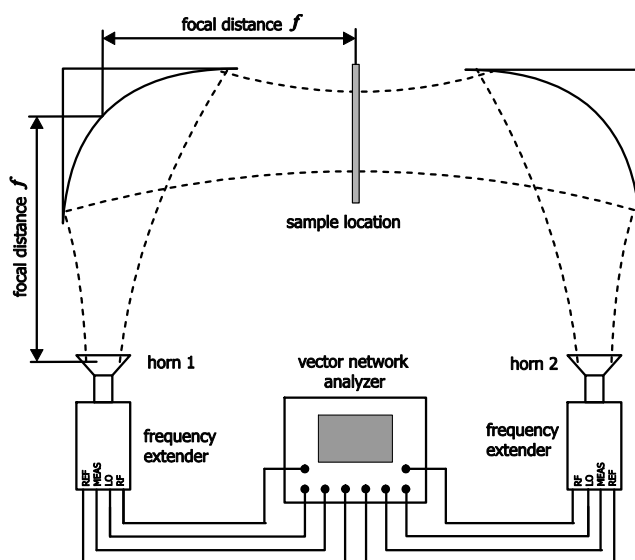

Fig. 3.2.4: Schematic overview of the quasi-optical measurement system.

In order to establish the missing traceability of VNA-based systems, a simple setup with standard gain pyramidal horn antennas together with a practical comprehensive calibration process and simple data extraction algorithm has been developed by PTB and CMI. The system, which uses compact-size mirrors to cover the wide frequency range from 50 GHz to 500 GHz and a reliable simple calibration method is used without need for precise positioning. The system consists of a commercial VNA and sets of waveguide frequency converters: 50-75 GHz, 75-110 GHz, 110-170 GHz, 140-220 GHz, 220-325 GHz and 325-500 GHz. The waveguide ports are connected to conventional rectangular horn antennas and two symmetrical parabolic mirrors are used to reduce the free-space transmission path loss (Fig. 3.2.4). The photograph of the system is shown in Fig 3.2.5.
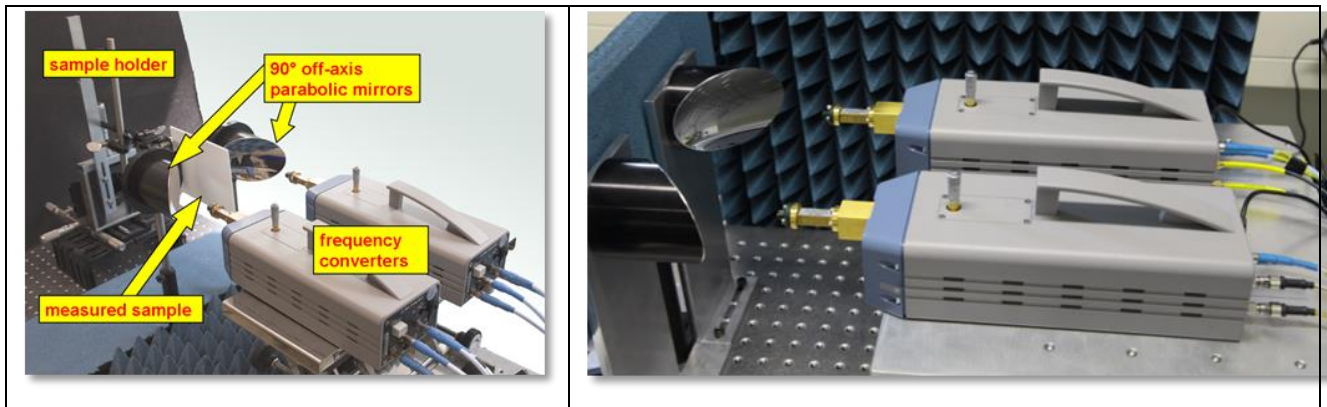
Fig. 3.2.5: Photograph of the free-space VNA spectrometer; first version (left) and second version (right) with improved mechanical stability.

The system topology and the shape and size of the mirrors must be designed to improve the measurement accuracy for the whole frequency range and optimise the cost and fabrication feasibility. Here two 90° parabolic off-axis mirrors are used to reduce the system size, cost and degrees of freedom of the adjustable parameters. Their distance to the antennas must be determined precisely to satisfy the plane-wave conditions on the material-under-test surface and to ensure maximum energy passing through for a further improved sensitivity. Horn antennas are symmetrically put at the focal-points distance (f) of the parabolic mirrors which are separated by a distance equal to $2f$ (Fig. 3.2.4).

A two-stage calibration process is performed. A calibration with waveguide standards in the reference plane of the frequency extenders' waveguide flanges was followed by a measurement on the empty horn-mirror system to move the calibration reference planes to the central beam waist (by de-embedding) and to correct for losses/ diffraction. Several calibration methods exist in free-space and most of them are very sensitive to the quality and the precise location/orientation of the "short" standard (equivalent of calibration methods known from guided structures). The "transmission-only" method is usually used for the sub-millimeter wave domain because reflection measurements are difficult at these frequencies. The calibration plane is shifted virtually from the VNA waveguide ports to the material-under-test surface. This represents the complete deembedding technique for which the overall scattering effects of the propagation path from the actual VNA ports to the material surface are evaluated experimentally. The key point is to evaluate the propagation path losses/diffraction by measuring the S-parameters of the empty setup which is supposed to be symmetrical (Fig. 3.2.6) and then repeating the same process with the material.

A simple method for permittivity extraction has been presented by PTB and CMI based on transmission coefficient measurements. Provided a plane wave propagates through a homogeneous flat sample slab with thickness L, the real part of the permittivity can be determined from the phase of the transmission coefficient T and the imaginary part from the magnitude of T. Multiple reflections inside the material slab must be taken into account. All the necessary formulas have been presented in a closed form suitable for a subsequent parametric error analysis. Several material slabs were measured and we report the results for six of them as representatives of thick and thin slabs as well as lossy and

Fig. 3.2.6: De-embedding of the S-parameters.

low-loss materials:

- Teflon (L = 2 mm)

- polyvinylchloride (PVC, L = 8 mm)

- glass (L = 2 mm, lossy)

- bor-crown glass (BK7, L = 500 µm, lossy)

- quartz (L = 500 µm)

- polymethylmethacrylate (PMMA, L = 4 mm).

The extracted real and imaginary parts of the permittivity are shown in Fig. 3.2.7.

Fig. 3.2.7: Extracted real and imaginary parts of the permittivity.

The simple method for VNA-based spectrometer calibration and data extraction method give comparable or better results as methods used in the past.

Traceability of Fourier-Transform THz systems

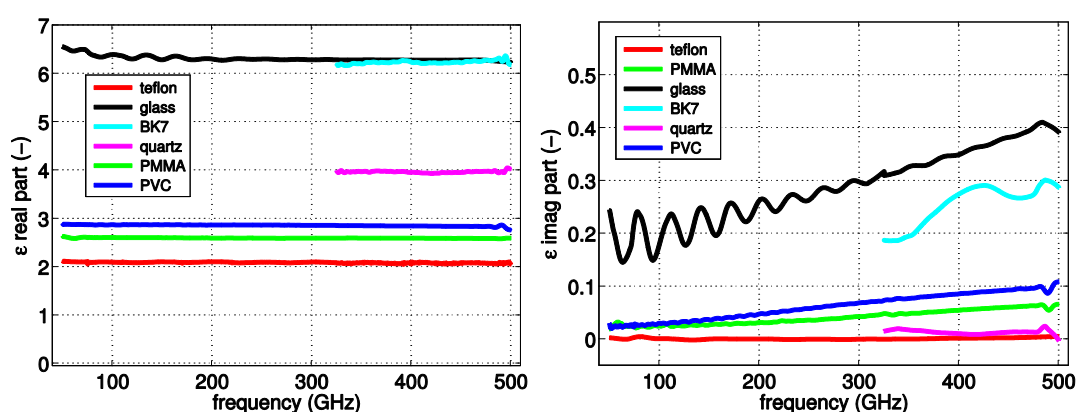Fourier-transform THz systems are the workhorse for measurements of the spectral properties of materials in the far infrared. E.g. precise emissivity measurements of thermal materials are import for many technical applications where thermal radiation sources are applied for heating purpose at any temperature. In order to determine this physical quantity in the far infrared, accurate transmission and reflection measurements have to be performed with a Fourier-transform THz spectrometer with known uncertainty.

Fig. 3.2.8: FT-MLS: optical setup at the THz beam line of the Metrology Light Source.

Three different THz radiation sources were tested as external THz radiation source of a Bruker VERTEX 80v vacuum FT-IR spectrometer: coherent synchrotron THz radiation at the Metrology Light Source (Fig. 3.2.8), monochromatic radiation of a FIR molecular gas laser and the broad band radiation of a high-pressure mercury discharge lamp. After a warm up time of one hour the discharge lamp delivered an output signal more stable in time than the coherent synchrotron THz radiation. Therefore the discharge lamp was used in a special configuration of the optimised setup in task 3.2.

The nonlinear power response of a FT-FIR spectrometer was determined at THz laser lines of the FIR molecular gas laser. The lowest nonlinearity was measured with a FIR DLATGS pyroelectric detector operated at room

temperature. The result of the DLATGS detector is shown for different entrance apertures of the Bruker FT-FIR spectrometer in Fig. 3.2.9.

The lowest nonlinearity (< 2 %) is achieved for the largest aperture (> 4 mm). Then no modulated radiation is reflected back into the interferometer by the metal entrance aperture which causes artifacts in the Fourier-transformed spectrum by higher order signal modulation generated by multiple circulation of diffracted THz radiation inside the interferometer of the FT-FIR spectrometer. As the red laser light of a He/Ne-Laser which is integrated in the interferometer is recorded parallel to THz radiation, the frequency accuracy of this FT-IR spectrometer is known with a relative uncertainty less than 2×10^{-6}. This is assured by the known absolute wavelength (632.816 nm) of this He/Ne-Laser which was verified before (Optics Express **22**, 2014, 25071-25083).
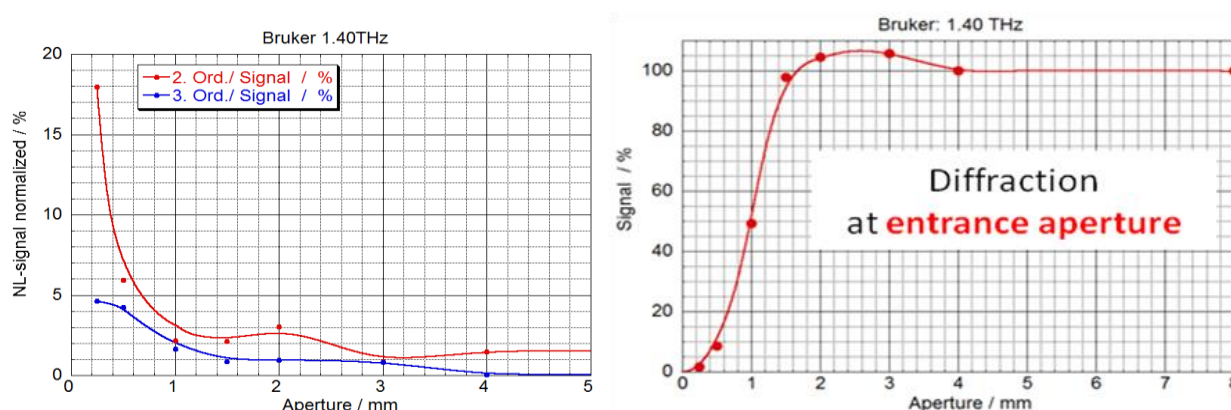

Fig. 3.2.9: Nonlinear response (left) and normalized signal of the DTATGS detector.

Spectrometer verification

Terahertz spectroscopy has been a well-established technique for the last two decades. Measurement of materials of different types such as foams, dielectrics, polymers, semiconductors, water charged materials, liquids, and others, have been published. These measurements cover a wide range of possible absorption coefficient and refractive index values. Well known characteristics of reference materials validated from the microwave to the infrared ranges can contribute to establishing the traceability of terahertz spectrometers.

Based on already published work, a well-defined list of traceable reference materials with known uncertainties for both absorption coefficient and refractive index of semiconductors, dielectrics, and polymers has been proposed. This is a prerequisite for a detailed uncertainty analysis of terahertz spectrometers and a way for the comparison of the performance of the different types of terahertz spectrometers described above.

The important characteristics of the reference materials are the refractive index and the absorption coefficient, or the permittivity since the complex refractive index is the square root of the complex relative permittivity for non-magnetic materials. Low absorption materials are suitable for transmission based spectrometers and high-absorption or high-reflection materials can be used for reflection based spectrometers.

The criteria for the materials selection were basically homogeneity and reproducibility from a sample to another, isotropy or well-defined anisotropy, market availability and high fabrication quality, long term stability, and possibly environment insensitivity. Selection also has been made in order to ensure wide enough ranges in terms of refactive index and absorption coefficient.

Table 3.2.1 below gives the thickness of each sample used in the work and a qualitative information on the surface rugosity. All the samples are disc shaped with 3" diameter.

Material	Sample thickness (µm)	Rugosity
Quartz	567	No
Borosilicate glass	479	No
Pyrex	575	No
Alumina	635	Yes
HR Si	400	Yes
TPX	2700	Yes
Parylene	20.56	Thin film

Table 3.2.1: Selected reference materials samples.

LNE carried out measurements with a commercial time-domain spectrometer and uncertainty calculations on the different samples, based on parameter sensitivity analysis. The values obtained (refractive index and absorption coefficient) are consistent with published data.

Table 3.2.2 below gives the measured refractive index and absorption coefficient and their uncertainties. They are compared against published data where available.

Material	Measured refractive index	Uncertainty ($k=2$)	Measured absorption coefficient (cm^{-1})	Uncertainty ($k=2$)	Up limit frequency (THz)	Published refractive index	Published absorption coefficient (cm^{-1})
Quartz	1.97	0.02	0 to 12	1.76	1.6	1.95	0 to 10
Glass BK7	2.5	0.02	0 to 100	5.84	1.1	2.5	0 to 100
Glass Pyrex	2.1	0.01	0 to 60	1.71	1.4	2.1	0 to 60
Alumina	3	0.15	0 to 16	7	1.7	-	-
HR Si	3.55	0.2	0 to 2,8	bad	1.7	-	-
TPX	1.46	0.01	0 to 0,8	0.8	1.6	1.46	0 to 1
Parylene	1.7	0.13	-	-	1.4	1.6	0 to 6

Table 3.2.2: Refractive index and absorption coefficient with uncertainty of the selected reference materials.

Summary

The objective to establish traceability of amplitude, phase and frequency for pulsed time-domain, vector network analysis (VNA) based and Fourier-Transform Infrared (FTIR) spectrometers and to develop reference materials for spectrometer validation has been met comprehensively. Traceability for the relevant quantities has been established for all three spectrometer types and materials for spectrometer verification have been chosen and were characterised.

3.3   Assessment of the performance of THz spectrometers by comparison of their uncertainty

This objective was to determine the uncertainty of spectrometers in the sub-THz and THz frequency range. In particular, the performance of existing scanning and spectroscopy systems was analysed quantitatively.

Uncertainty analysis of VNA spectrometers

The traceability of VNAs is dependent mainly on calibration standards and the accuracy of characterisation of their physical dimensions. Currently the s-parameter traceability is achieved via precision dimensional measurements of waveguide (or coaxial) sections and is commercially offered up to 110 GHz in 1.0 mm coaxial line by several NMIs. First attempts have been made to extend this range, e.g. traceability of 140 GHz to 220 GHz band for WR-05 waveguide or on-wafer measurements using WR-1.5 waveguide in the frequency range of 500 GHz to 750 GHz. Various calibration methods such as Thru-Reflect-Line (TRL), Line-Reflect-Line (LRL) or Thru-Short-Match (TSM) are used. Detailed uncertainty analysis for vector network analyser measurements in WR1.5 rectangular waveguide (500 GHz to 750 GHz) is given in literature. In the VNA spectroscopy, however, the full 2-port VNA calibration is often not necessary since only transmission and reflection of a sample are determined. Measurements of the wall dimensions of the apertures of the waveguides are made using coordinate measuring machines with typical dimensional uncertainty of about 0.4 µm. The overall uncertainty budget for conventional vector network analysers is described in literature, yet needed to be extended since precision transmission lines required for the calibration are not easily available at sub-millimetre wavelengths. For frequency extension of VNAs up to 500 GHz, novel waveguide calibration standards had to be designed and characterised and additional uncertainty components had to be taken into account.

As discussed in literature, the sub-millimetre system accuracy is limited by the coupling of the antennas (or probes) and the output power of the frequency extender heads. The accuracy is also decreased by impedance mismatch and power dropout in the frequency extender heads. Uncertainty of material parameters calculated from the measured scattering parameters is moreover influenced by the mechanical set-up of the system (sample alignment, sample thickness, air refractive index etc.). The uncertainty of the abovementioned effects on the measurement accuracy was studied for this objective.

Uncertainty Analysis of FT-FIR spectrometers

The different spectrometer types available for the THz frequency range have in common that they are used to determine the absorption and reflection coefficient of a variety of different samples. Depending on the type of sample, very different results have been obtained for different spectrometer types. Among the spectrometers that can be used around 1 THz and lower frequencies are Fourier-Transform far infrared (FT-FIR) spectrometers. At the long wavelengths in the far infrared spectral range a well characterised uncertainty budget did not exist so far.

Based on the work performed within the second objective that established traceability for the power response and frequency of FT-FIR spectrometers, an analysis was performed for spectrometers with different light sources that are used to illuminate the sample. An optimal spectrometer setup was identified. The error sources were investigated in detail including influences from the sample and the data extraction method. An uncertainty budget was set up that allows quantifying the performance.

A commercial FTIR spectrometer (Bruker Optics – Vertex 80v) was adapted at PTB Berlin for measuring in the THz gap (see Fig. 3.3.1). This instrument is capable of measuring from about 200 GHz to about 6 THz with a frequency resolution of about 67 GHz.
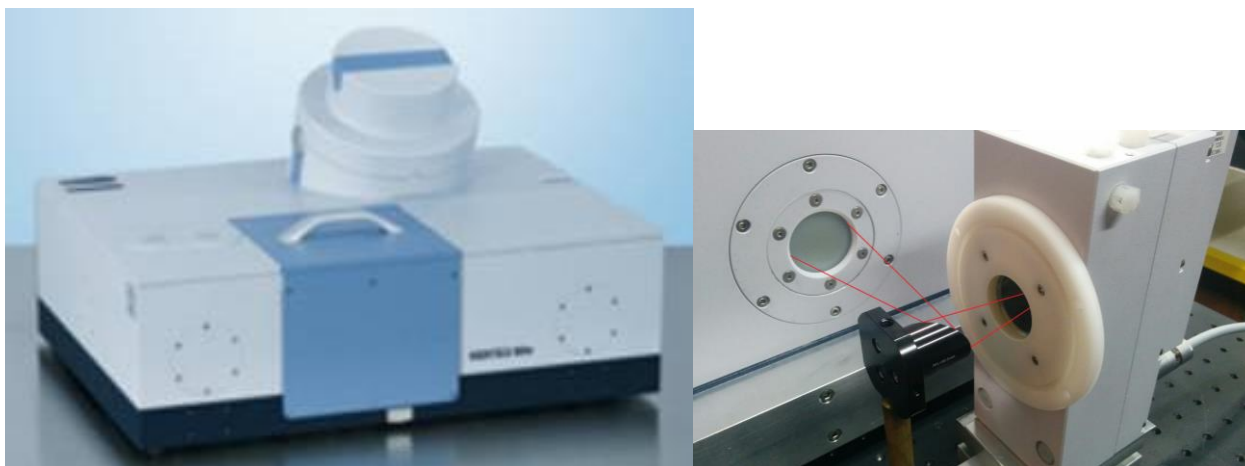
Fig. 3.3.1: The PTB FTIR spectrometer with a high power mercury discharge (right) lamp as external THz source.

An optimised optical setup with a high pressure mercury lamp as powerful external THz radiation source and a DLaTGS pyroelectric THz detector at room temperature was used to measure the transmittance and reflection of the three travelling standards. The samples had to be tilted off normal incidence in order to avoid spectral artefacts by specular reflection of the modulated THz radiation back to the interferometer. In order to get low noise spectra after Fourier-transformation an average of 256 scans was recorded. The frequency accuracy of this a FT-IR spectrometer is assured by a red He/Ne-Laser of known absolute frequency which is integrated into the interferometer.

The thin samples allowed the extraction of the refractive index from the frequency position Fabry-Perot fringes of the transmission and reflection spectra with low uncertainty. The exact interference order is easily counted because the FSR of a 0.5 mm thin sample is only about half the lower limit of the recorded spectra, e.g. as seen by the transmission spectrum of the quartz sample (Fig. 3.3.2).
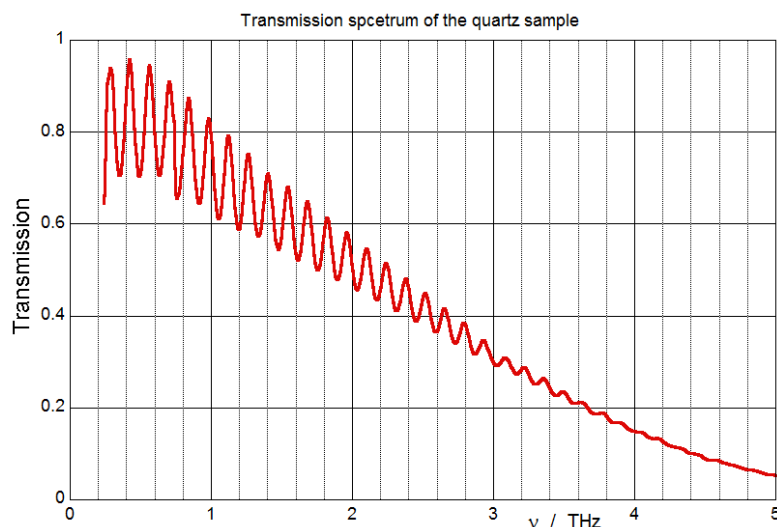

Fig. 3.3.2: The PTB FTIR transmission spectrum of the quartz travelling standard.

The absolute known frequency positions $\nu(m)$ of both the maxima (integer order: m) and the minima (half integer order: m+1/2) are used to calculate the frequency dependant refractive index $n(\nu)$ from the known thickness d, the tilt angle δ:

$$n(\nu) = m*c / (2d * \cos(\delta) * \nu(m)) \qquad (2)$$

For a given thickness d, the uncertainty of n(ν) is simply given by two terms:

- the uncertainty of maxima /minima frequency position determination in the recorded spectra;
- the uncertainty of the tilt angle.

Moreover, there is a fixed uncertainty contribution of the min/max position: 0.003 for quartz and pyrex. As BK7 is strongly absorbing above 600 GHz the only two evaluable maxima and minima yield just a single value at 400 GHz for the larger refractive index of BK7 with an increased uncertainty contribution of 0.03. The tilt angle has a standard uncertainty of 1 degree for all samples. The resulting relative standard uncertainty of $\cos(\delta)$ is: 0.003.

The transmission spectra are also used to extract the spectral absorption. First of all, only the maximum values are selected in the transparent region with visible Fabry-Perot fringes. Then an interpolating curve T is calculated from these maxima. Outside this frequency interval, the transmission is <8%, i.e. no signal modulation due to interference by standing waves inside the sample is visible in the data.

Therefore the interpolating curve T is extended simply by the measured data for $T<0.08$. The absorption is the calculated $abs = -\ln(T)$.

The uncertainty of the absorption is estimated to 4% for quartz and pyrex. As BK7 has a much higher refractive index and is already at 1 THz strongly absorbing and therefore the transmission curve could not be precisely measured. The resulting uncertainty of the calculated absorption is 13 %.

The extinction coefficient κ is calculated with the known thickness d and the verified frequency ν from the absorption abs:

$$\kappa = abs^* \, c \, /(d \, * \, 4 \, \pi^* \, \nu) \tag{3}$$

As all conversion factors of the absorption are precisely known, there is the same uncertainty for calculated extinction coefficient κ as for the measured absorption abs.

Uncertainty Analysis of THz TDS

Considering the outcomes of earlier tasks that should provide the traceability for TDS measurements, and using the reference materials selected for spectrometer validation, a detailed measurement uncertainty budget was established.

Experiments included both low and high absorption materials for which absorption and reflection coefficients are measured, respectively. For this reason the TD spectrometer was realised both in transmission configuration and reflection configuration and the covered frequency range was from 0.1 THz to 2 THz with a frequency resolution of about 29 GHz. A picture of the system is shown in Fig. 3.3.3.
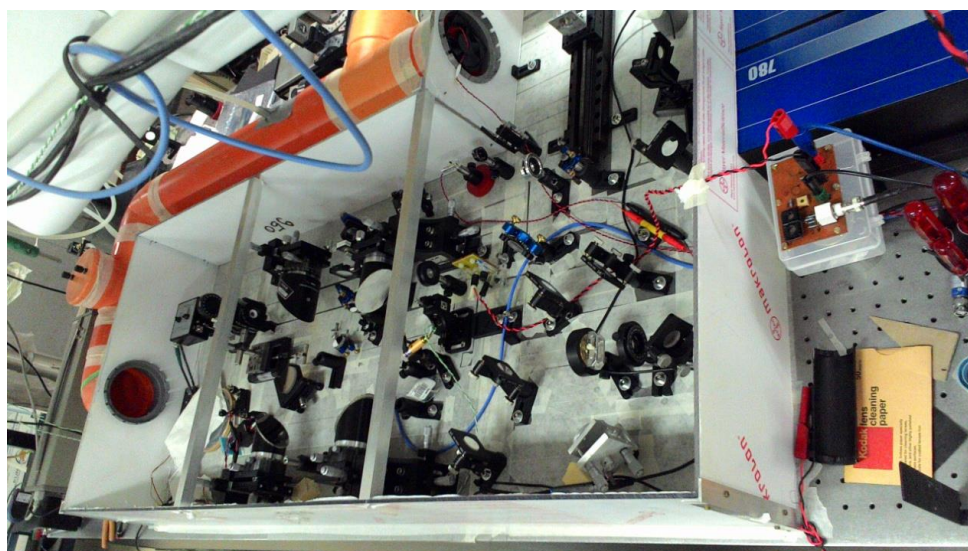
Fig. 3.3.3: Picture of the INRIM THz-TDS.

Comparison of different spectrometer types

The aim of this task was to compare the performances of three different measurement systems in measuring the reflection and absorption coefficient of some materials in the THz gap. Such materials could be selected among the list provided by LNE in WP2 considering the material availability, ease of handling, shaping, preparation and storage. The choice was agreed upon among INRIM, PTB and LNE.

Long-term stable travelling standards such as semiconductor materials, dielectric materials and polymers were circulated between INRIM and PTB on the base of a protocol to be established. Measurements were performed in a selected frequency range common to the three spectrometers involved.

The measurand chosen for this exercise was the complex refractive index of the materials under test. In particular, participants had to measure the refractive index and the extinction coefficient that are the real and the imaginary part of the complex refractive index, respectively.

The travelling standards have been provided by LNE. The material they are made of were chosen by LNE itself from a list prepared previously in order to ensure wide enough ranges in terms of refractive index and extinction coefficient. Selected materials were quartz, pyrex and BK7. The travelling standards had the shape of a 100 mm diameter disk for quartz and 76 mm diameter disks for pyrex and BK7. The disk thicknesses as mechanically measured at INRIM are summarised in Table 3.3.1.

Material	Thickness / μm
BK7	545 ± 1
Pyrex	570 ± 1
Quartz	549 ± 1

Table 3.3.1: Thickness of the travelling standards.

Comparison between TDS and VNA, in the lower part of the THz gap band (Below 500 GHz), has been performed on two samples only (quartz and BK7), PTB not having measured the pyrex travelling standard. The comparison between TDS and FTIR has been made among measurements concerning all the travelling standards, but the FTIR measurement of the refractive index of BK7 has been made at the frequency of 400 GHz only, due to high material absorption at higher frequencies.

As it can be seen from Fig. 3.3.4 (quartz results), FTIR measurements span over the widest frequency range. The band covered by VNA is the smallest one while TDS lays in the middle. TDS and FTIR have roughly comparable refractive index uncertainty while VNA has the largest. On the counterpart, TDS has the largest extinction coefficient uncertainty and the FTIR spectrometer clearly outperform the other instruments. Anyway all the measurements, regardless the instrument used, are well compatible.

In Fig. 3.3.5 (BK7 results), measurements results for the BK7 travelling standard are shown. For this sample, the extinction coefficient is about ten times higher than that of the other two. It comes up that the INRIM TDS is the most suitable instrument for characterising this kind of materials, being it able to measure up to 1.1 THz with the lowest uncertainty. FTIR is severely limited by the material absorption while VNA based spectrometer has larger uncertainty for the refractive index and slightly lower for the extinction coefficient but it is limited by its frequency coverage. The comparison has positive outcome being all the measurements compatible.

The pyrex travelling standard has been measured by PTB with the FTIR spectrometer only. Results are in Fig. 3.3.6 and they are, again, well compatible. As already pointed out, FTIR has wider frequency coverage with respect to TDS. Refractive index uncertainty is not very different between the two systems while the extinction coefficient one is in favour of the FTIR spectrometer.
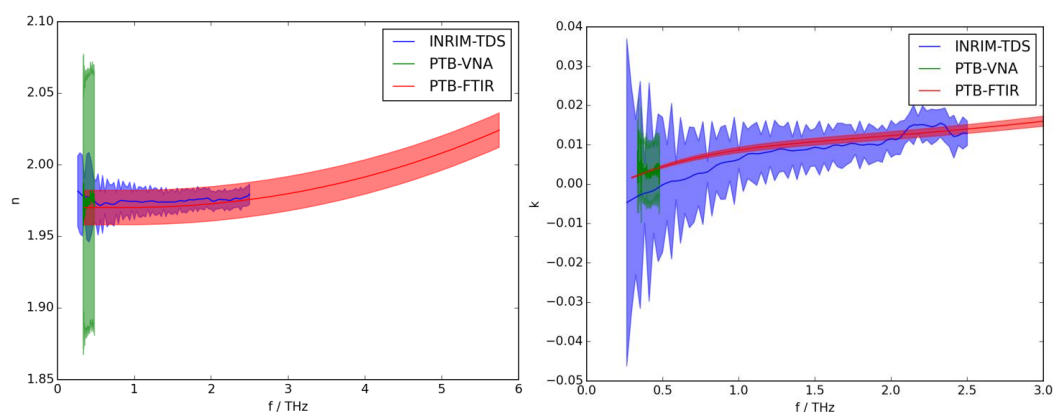

Fig. 3.3.4: Comparison of measurement results for the quartz travelling standard.
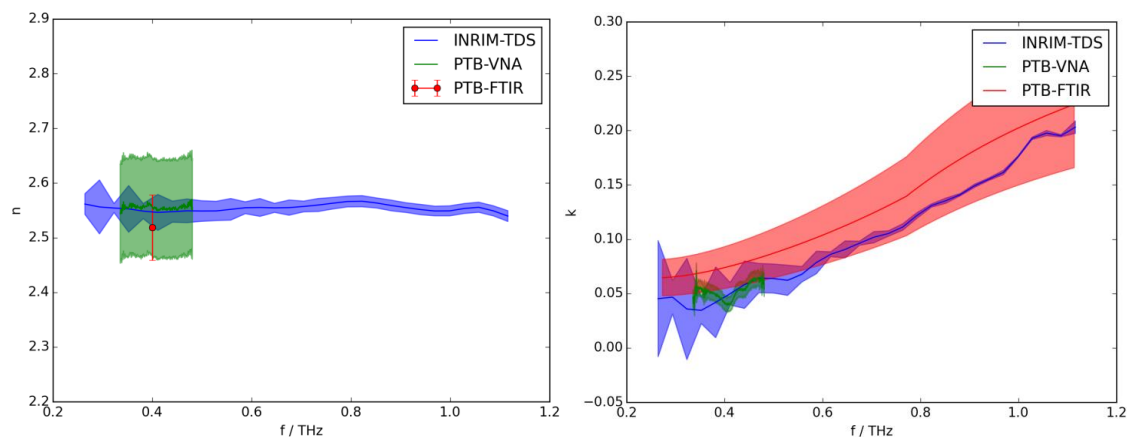
Figure 3.3.5: Comparison of measurement results for the BK7 travelling standard.
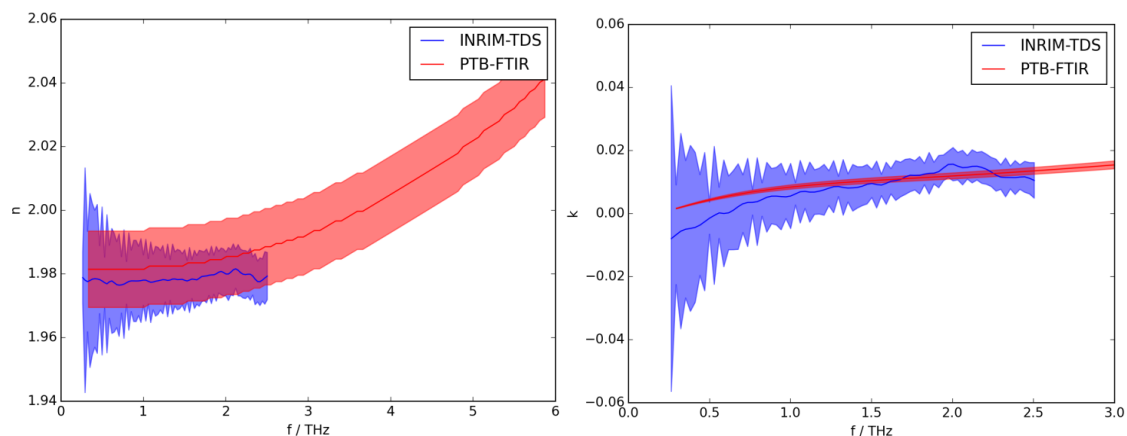

Figure 3.3.6: Comparison of measurement results for the pyrex travelling standard.

While the measurement of the refractive index did not cause particular problems, the measurement of the extinction coefficient was more critic. In practice, its value was extremely low for two of the tree samples and it was very difficult to measure the absorption of a material that is almost transparent at the lower frequencies of the considered frequency band, indeed (below about 800 GHz). At these low frequencies, the VNA based spectrometer performs better than TDS but the FTIR spectrometer is the best choice for extinction coefficient measurements. On the other hand, BK7 has higher extinction coefficient, about ten times higher with respect to quartz and pyrex. Therefore, for this material, good measurements have been possible in all the range of interest with the TDS also.

Conversely TDS showed better performances in measuring the refractive index with respect to the VNA in the band of overlapping and similar performances to the FTIR. It is worth noting that, while the FTIR spectrometer has the widest frequency coverage, for what concerns the BK7 sample, the FTIR has not been able to measure its refractive index in all the frequency band due to its high absorption. A measurement at a single frequency (400 GHz) has been performed, actually. FTIR measurements of the BK7 extinction coefficient have high uncertainty also. VNA based spectrometer turned out to be a good choice for measurement in the lower part of the THz gap and below while FTIR spectrometers are more suitable for measurement of the extinction coefficient in the band of interest and beyond. THz Time Domain spectrometers turned out to be the best choice for measuring the refractive index in the whole band from about 100 GHz to about 2.5 THz. At lower frequencies VNA based spectrometers have to be preferred while FTIR ones are needed beyond 2.5 THz.

Tables 3.3.2, 3.3.3 and 3.3.4 show a comparison of the measurements for the three samples at the common frequency of 400 GHz.

Instrument	Refractive index	Extinction coefficient
INRIM TDS	1.98 ± 0.03	-0.002 ± 0.026
PTB VNA	1.98 ± 0.09	0.003 ± 0.008
PTB FTIR	1.970 ± 0.006	0.0032 ± 0.0003

Table 3.3.2: Comparison of Quartz measurements at 400 GHz.

Instrument	Refractive index	Extinction coefficient
INRIM TDS	2.55 ± 0.03	0.05 ± 0.01
PTB VNA	2.56 ± 0.09	0.042 ± 0.007
PTB FTIR	2.55 ± 0.06	0.07 ± 0.02

Table 3.3.3: Comparison of BK7 measurements at 400 GHz.

Instrument	Refractive index	Extinction coefficient
INRIM TDS	1.98 ± 0.02	-0.005 ± 0.021
PTB VNA	---	---
PTB FTIR	1.982 ± 0.006	0.0031 ± 0.0002

Table 3.3.4: Comparison of pyrex measurements at 400 GHz. PTB did not measure this standard with the VNA.

Summary

The objective to assess the performance of pulsed time-domain, VNA-based and FTIR spectrometers, by comparison of their uncertainty, has been met comprehensively. The uncertainty analysis has been performed for the three spectrometer types and comparison measurements have been made and were evaluated.

3.4 Assessment of the radiated power flux densities of microwave and THz security scanners and dosimetric assessment based on numerical skin models and phantoms

The objective was to define experimental and modelling procedures to evaluate human exposure to the EM fields emitted by millimetre-wave and THz scanners. The activity has been organised into three sections. The first one was focused on the characterisation of microwave and THz scanner emissions, traceable to SI units, in order to provide reliable inputs for the human exposure assessment. A second activity was devoted to the development and validation of advanced computational tools for the evaluation of energy deposition and temperature elevation in human tissues consequent to the EM irradiation. Finally, on the basis of the tools preliminary developed, human exposure to actual body scanners has been performed, allowing a preliminary assessment of related safety issues.

Characterisation of microwave and THz scanner emissions

In order to characterise the field emissions of microwave and THz scanners, traceable to SI units, a preliminary analysis has been done to calibrate the detectors and to define the most appropriate measurement procedure.

Microwave scanners are characterised in terms of power flux density emission S, defined as,

$$S = \frac{P}{A_{eff}} = \frac{P}{G \cdot \frac{c^2}{4\pi f^2}} = \frac{4\pi f^2}{G \cdot c^2} P \quad [\text{W/m}^2], \tag{4}$$

where P is the measured power, A_{eff} is the effective antenna area (aperture), G is the far-field antenna gain, f is the frequency and c is the speed of light. It must be remarked that when measurement are being made at a distance L, in the near-field zone of the receiving antenna ($L << D^2/\lambda$, where D is the maximum overall

dimension of the antenna and *λ* is the free-space wavelength), then the far-field antenna gain cannot be used without introducing an error.

Three microwave scanners have been measured by PTB (L3 Provision 100 and Smith Detection Eqo) and LNE (L3 Provision 2). Both L3 Provision scanners have two moving masts around the scanned volume, both containing transmitting and receiving antennas disposed vertically, so that the positioning scheme of the receiving antenna is identical for these two scanners. The Eqo scanner has a fixed transmitter/receiver antenna that illuminates a passive matrix panel, through the scanned volume. For the general public, the scans involve a brief exposure time. However, for occupational situations during manufacturing, testing and installation, repeated exposures or extended exposure durations may occur.

Since the access to the full control of the scanner is usually not given by the manufacturer, the laboratory characterisation has been done to get the maximum possible power level, and then the positioning scheme will necessarily consist in searching the position and direction that gives the highest detectable signal. Unfortunately, the low levels noticed during the tests involve to position the antenna near the emitting mast, at few centimetres (see for example Fig. 3.4.1 a).

The typical measurement system includes a receiving antenna connected to a spectrum analyser (Fig. 3.4.1 b). The uncertainty budget is mainly based on the calibration of the different element of the measurement chain: starndard horn antenna, connecting cable and spectrum analyzed. As an example, for the measurement chain used for the L3 Provision 2 scanner we have:

The measured antenna gain: 18.45 dBi ± 0.26 dB

The measured cable attenuation: -10.17 dB ± 0.4 dB

Calibration of the spectrum analyser (see Table 3.4.1). The uncertainty is 0.4 dB.

The repeatability observed on the trigger threshold maximum is 0.5 dB for four repeated measurements.

In this example, the final level obtained for the power flux density is $S = 5.7 \cdot 10^{-4}$ W/m², which is far below the guidelines limits.
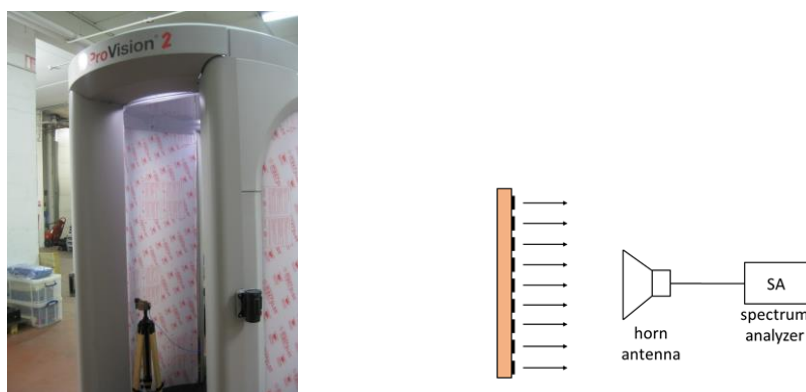
Fig. 3.4.1: (a) Positioning of the receiving antenna in the near-field zone for L3 Provision 2 scanner; (b) scheme of the power flux density measurement.

Level (dBm)	Correction (dB)
-56	-0.29
-55	-0.32
-54	-0.28

Table 3.4.1: Calibration of the spectrum analyzer.

The emission measurements on THz security scanner sources can be done with a Thomas Keating Power Meter™. The power meter consists of a large photo-acoustic detector with a sensitive area greater than the maximum beam diameter of 3 cm. It is placed in the THz beam under the Brewster angle of 55.5° in order to

prevent reflection losses and standing waves. The detector consists of a closed gas cell formed by two closely spaced parallel windows made of polymethylpentene (TPX, Mitsui Chemicals, Tokio, Japan). A thin metal film in the gap absorbs part of the chopped THz beam passing through the cell and heats the gas. The resulting pressure modulation is detected with an acoustic detector. The overall measurement uncertainty (k=2) for the beam power is estimated to be 14 %.

Two different emitters of THz radiation were investigated: (a) a photoconductive THz antenna used in the handheld scanner investigated in REG UMR, here considered to be a representative pulsed source, and (b) an optically pumped laser system with intra-cavity THz generation, here considered as typical strong THz emitter. Moreover, a representative electronic continuous-wave THz source at 350 GHz was considered as reference source of the passive THz scanner in REG TUB.

1) Handheld scanner

The THz emission of the fibre coupled antenna has been collimated with a spherical lens with a focal length of 150 mm and then has been focused with a spherical lens with a focal length of 75 mm to match the aperture of the detector. The detector was a Golay cell that had been referenced with the THz source at PTB.

The beam profile of the resulting collimated beam was measured with the knife-edge method. From the analysis of the measured raw data, the beam diameter (FWHM) has been derived as 37.3 mm. From the small deviation of the fit to the raw data by an inverse error function, the beam shape is found to be nearly Gaussian. From the measurement of the beam profile that is presented in the preceding section, the total THz output power is derived based on the fact that the detector was a Golay cell that had been referenced with the THz source at PTB. On the basis of this referencing procedure the total THz output power results as 0.073 nW.

2) TECSEL

The THz emission of the TECSEL has been collimated with a cylindrical lens with a focal length of 3 mm (Fig. 3.4.2). The beam profile of the resulting collimated beam was measured with the knife-edge method in horizontal and vertical direction, respectively.
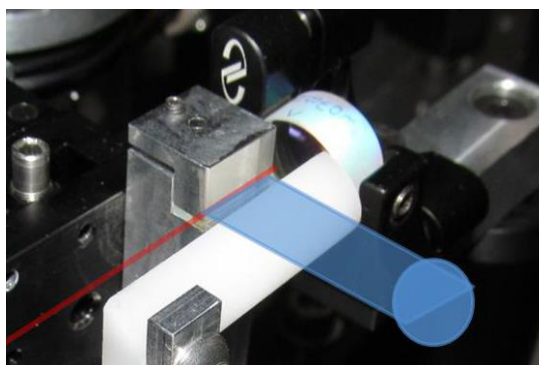

Fig. 3.4.2: Photograph showing the nonlinear crystal inside the cavity of the TECSEL. The cylindrical collimating HDPE lens having a white color is visible positioned in front of the nonlinear crystal. A red line is introduced in the photograph to represent the cavity mode axis of the TECSEL. The direction and shape of the emitted THz radiation is schematically represented in blue.

From the analysis of the measured raw data, the beam diameter (FWHM) in horizontal and vertical direction has been derived as 12.4 mm and 10.9 mm, respectively. From the small deviation of the fit to the raw data by an inverse error function the beam shape is found to be Gaussian.

From the measurement of the beam profile, that results in a Gaussian shape although with slight different beam diameters in horizontal and vertical directions, and from the measurement of the total THz output power, under the assumption of a perfect Gaussian shape, the power density can be calculated. Fig. 3.4.3 shows a false color plot of the power density. The power density ranges up to 1.3 $\mu W/cm^2$ for the total power of 2 μW used in this measurement, which is not at all the maximum output power of the TECSEL.
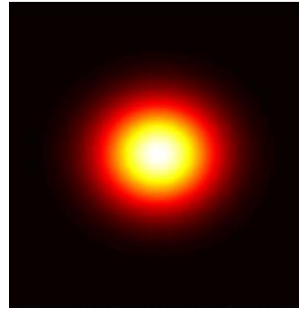
Fig. 3.4.3: False color representation of the calculated output power density from the measurement of the beam profile. The representation covers an area of 40 mm times 40 mm. The color codes power density ranges up to 1.3 µW/cm^2 for the total power of 2 µW used in this measurement.

Models for energy deposition in tissues and temperature elevation

Two mathematical models have been developed and tested by INRIM to predict energy deposition and temperature elevation of tissues radiated by EM waves generated by microwave and THz scanners. A first approximated model was developed under the simplifying assumption of considering a plane wave incident to a stratified model of human skin. Despite its simplicity, this model allowed a wide analysis of the influence of tissue properties (stratification and dielectric properties of skin), considering both 3-layer and 5-layer models. In particular, the stochastic analysis has put in evidence the effect of properties (due to the uncertainty in tissue characterisation and subject variability) on the temperature elevation. A complete analysis is reported in L. Zilberti et al., Bioelectromagn. **35**, 314 (2014).

In a second version of the model, the effect of the focused beam has been included in order to represent in a more realistic way the characteristics of the source. Human tissue has been here modelled as a stratified cylinder divided along its axis (z-axis) into three homogeneous layers, namely skin, subcutaneous adipose tissue (SAT) and muscle, disregarding effects due to tissue microstructure (e.g. sweat gland ducts). The muscle depth is assumed to be larger enough (40 mm), so that its artificial boundary does not alter the results. The values of the skin and SAT layer thickness and of thermal and electrical tissue parameters are summarised in Table 3.4.2 for 0.1 THz.

		5-Layer	**Equivalent 3-Layer**
Thickness (mm)	SC	0.015	
	Epidermis	0.035	1.15
	Dermis	1.1	
Relative permittivity ε_r	SC	2.4	
	Epidermis	3.2	6.1
	Dermis	5.8	
Electrical conductivity σ (S/m)	SC	0.0001	
	Epidermis	1	34
	Dermis	39	
Thermal conductivity λ (W/(m K))	SC	0.21	
	Epidermis	0.21	0.34
	Dermis	0.35	
Perfusion coefficient h_b (W/(m^3 K))	SC	0	
	Epidermis	0	6466
	Dermis	6760	
Heat capacity per unit volume c_V	SC	3.6	
	Epidermis	4.32	3.39
	Dermis	3.78	

Table 3.4.2: Electrical and thermal properties of the tissue at 0.1 THz.

The model allows the computation of time-spatial distribution of temperature elevation (θ), given the characteristic of the incident wave, the exposure time and the properties of the human tissues. As an example, Fig. 3.4.4 compares the results computed at 0.025 THz and 1 THz in terms of diagrams of θ along the beam axis and of chromatic maps in the *r-z* plane at *t* = 1 s and *t* = 8 s. The diagrams of Figs. 3.4.4 (a) and (b) put in evidence how at the end of the exposure time (*t* = 1 s) the highest frequency gives rise to the highest θ value, but its effect is significant only for deepness lower than 1 mm, whereas at 0.025 THz an appreciable temperature elevation is found up to *z* = 3 mm. After the radiation switch-off, the heating propagates mainly toward the internal tissues (the radial diffusion is significantly lower) and the peak value of θ quickly decreases, as in the maps of Fig. 3.4.4 (b), (c), (e) and (f). More results can be found in O. Bottauscio et al., IEEE Trans. on Magn. **51**, 7400504, (2015).

Results of simulations have been tested by comparison with in-vitro measurements, performed on suitable phantoms made of gel which mimics the dielectric properties of human skin. In particular, LNE developed phantoms based on two recipes. The first one (Recipe 1) is composed of (distilled) water and a polysaccharide type powder with commercial name TX151. A gum-like material is easily obtained when mixing the powder in the water.The optimised weight proportions are: Water: 75 % and TX151: 25 %. The second recipe (Recipe 2) is based on water, a lipid element, and a protein element obtained from porcine skin gelatin. It needs also the use of an emulsifying (Intralipid). The optimised weight proportions are: Water: 56 %, Sunflower oil: 12 %, Intralipid 12 %, Gelatin 20 %.
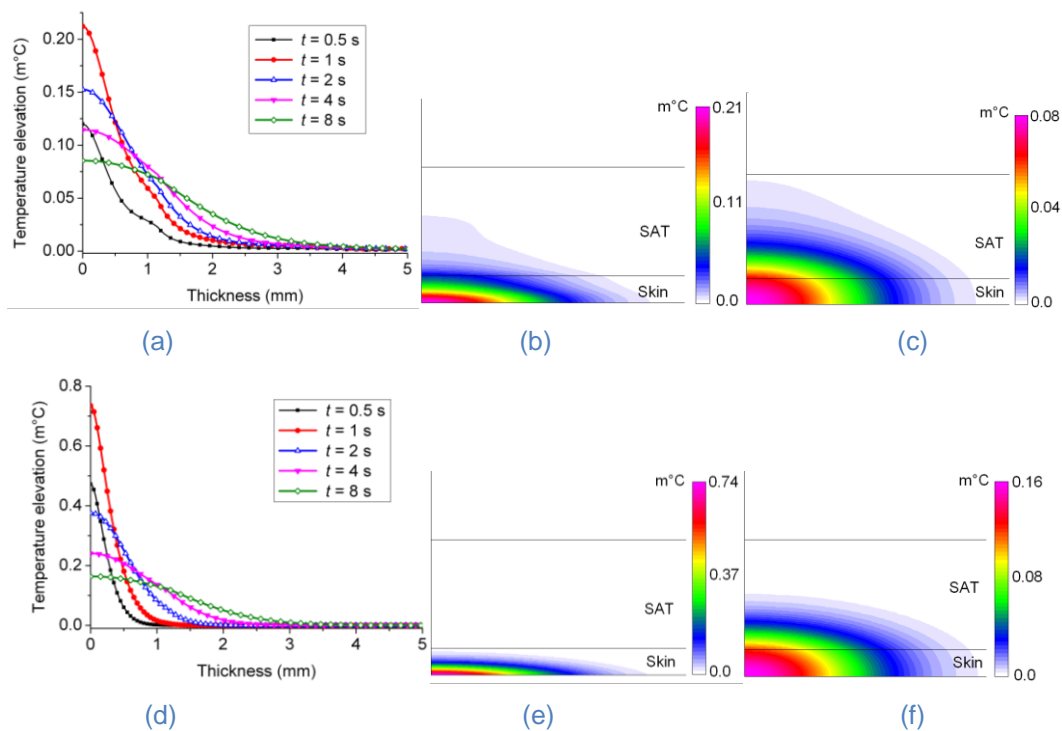

(a) (b) (c)

(d) (e) (f)

Fig. 3.4.4: Distribution of temperature elevation at 0.025 THz (upper diagrams) and 1 THz (lower diagrams). Diagrams of θ versus z at the symmetry axis for different time instant (a and d). Maps of the temperature elevation on a r-z plane at t = 1 s (b and e) and t = 8 s (c and f).

The laboratory experimental set-up for phantom irradiation was developed at PTB, using a standard-gain horn antenna to provide a Gaussian beam and an infrared camera to monitor the temperature variations on the phantom surface. Fig. 3.4.5 shows thermal images taken before and after the exposure to a nearly Gaussian beam at 35 GHz with a maximum power density of 40 mW/cm^2 ± 20%. The measurements after illumination are taken after 180 s, 450 s and 900 s. Temperature elevations are extracted from the images after subtraction of the background noise measurement (image of the sample without illumination), which is in the order of 0.5 K. Taking into account the capabilities of the infrared camera, the thermal stability of the

experimental environment and the limited homogeneity of the gel phantoms, we estimate an expanded measurement uncertainty for the extraction of temperature elevation to 0.2 K (k = 2).
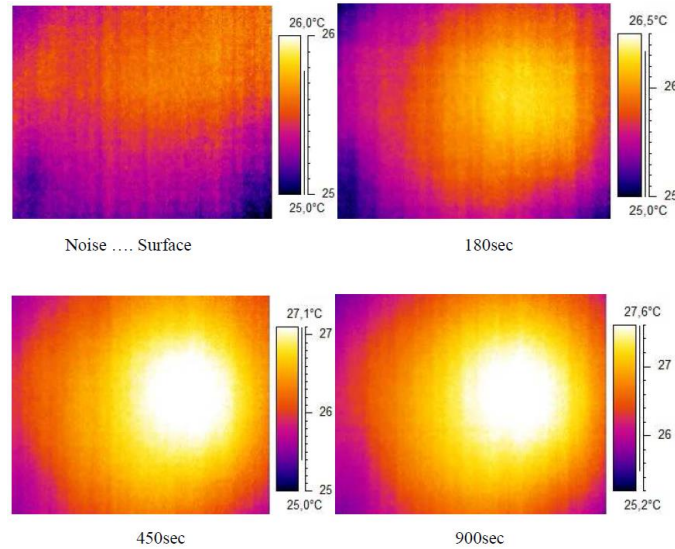

Fig. 3.4.5: Thermal images of the skin phantom after illumination with 35 GHz radiation of nearly Gaussian shape with maximum power density of 40 mW/cm^2 and a beam waist of $w_0 \approx 2.0 \dots 2.5$ cm for different illumination times between 0 s and 900 s.

Fig. 3.4.6 shows the comparison of simulations with measurements for two different values of the heat transfer between phantom and surrounding air (h_{amb}) which we assumed to be realistic. The simulated temperature elevations are still subject to a large uncertainty. The main contributions to this uncertainty are the antenna input-power (which is in the order of 20% for k = 2), the parameters of the approximated Gaussian beam, and the uncertainty of thermal and electrical parameters of the gel phantom. More details can be found in A. Kazemipour et al., 40th Intern. Conf. on Infr., Millim., and THz Waves, August 2015, Hong Kong (China).
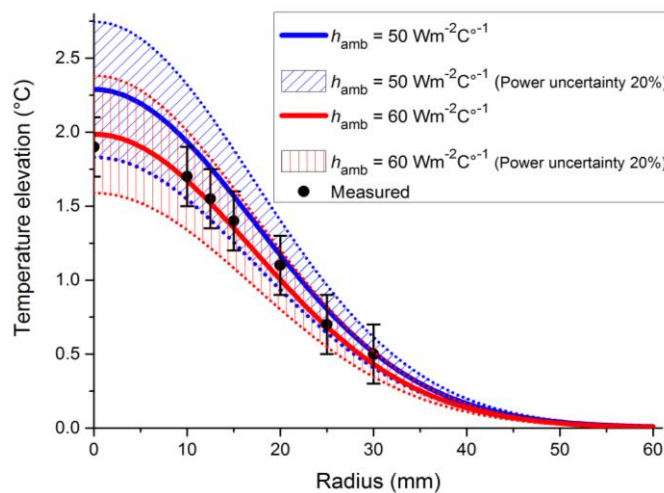

Fig. 3.4.6: Simulated temperature increase in comparison to the measured values extracted from the thermal image.

Assessment of human exposure to microwave and THz scanners

The computational tools have been finally applied to estimate the temperature elevation due to the exposure of human tissues to the electromagnetic field radiated by real body-scanners, whose features (frequency f and surface power density p) have been detected experimentally by PTB.

Two exposure scenarios have been considered:

1) Scenario 1 (representative for scanner QPS 100, by R&S): f = 75 GHz, p = 0.63 W/m^2

2) Scenario 2 (representative for scanner EQO, by Smith Detection, and also for scanner L3, by ProVision, which works almost at the same frequency but with lower power density): f = 24 GHz, p = 0.30 W/m^2

In order to get a conservative result, the exposure duration has been set to 10 s for both cases.

Two tissue models have been considered, simulating respectively the skin (model A) and the eye (model B), whose main characteristics are:

a) Model A: skin (1 mm), SAT* (3.5 mm), muscle (infinite)

b) Model B: cornea (0.6 mm), lens (4 mm), umor vitreo (20 mm), sclera (1.3 mm) , muscle (infinite)

The dielectric properties (electric conductivity and permittivity) and the thermal properties (thermal conductivity, specific heat capacity and perfusion coefficient) have been set for all materials according to the database developed by IT'IS Foundation (available at: http://www.itis.ethz.ch/virtual-population/tissue-properties/database/).

Results are reported in Table 3.4.3. For all cases (given by the combination of an exposure scenario with one of the tissue models), the absolute maximum temperature elevation takes place at the interface with the external air (hence, in the skin layer for model A and in the cornea for model B), at the final instant of the active exposure (i.e. after 10 s). For the deeper tissues, owing to thermal diffusion, the local maximum temperature elevation occurs later (when the electromagnetic radiation has been already switched off), but always at the interface with the adjacent (more external) layer.

Case	Maximum temperature elevation (m°C)
1A	0.54
1B	0.21
2A	0.15
2B	0.13

Table 3.4.3: Maximum temperature elevations.

Summary

The objective to assess the radiated power flux densities of different types of microwave and THz scanners, and to use the results for realistic dosimetry, by development of numerical skin models and phantoms, as a basis both for performance and safety evaluation of such systems, has been met completely. Radiated power flux density measurements have been performed on a variety of systems. The results have been used as input for numerical calculations of the heat transfer into human skin. The results have been verified successfully with thermographic measurements on skin phantoms.

4 Actual and potential impact

This project has substantially improved microwave and THz measurement accuracy and reliability, making these technologies readily accessible for security applications.

Industry/financial impact:

For the first time, a range of methods are now available for industrial users and research laboratories to calibrate THz instruments against measurement unit definitions:

- PTB has set up a new THz detector calibration service resulting from the detector radiometry implemented at additional frequencies. This is the first worldwide calibration service for a wide range of THz detectors at distinct frequencies between 1 THz and 3 THz. It enables every laboratory needing traceability to the SI units to establish an unbroken traceability chain using a suitable detector. The calibration service offered by PTB had already been used more than 20 times by the end of the project, by manufacturers and research institutions from China, Japan, USA, Russia, France and Germany.

- SFI Davos now offers a room-temperature radiometer commercial product. The product was developed in cooperation with PTB. The radiometer allows companies and research institutes to easily establish traceability for amplitude measurements above 1 THz.

- New pyro-electric detectors, to be used as calibration transfer standards, can be purchased from SLT GmbH.

This project has made fundamental contributions to improving the accuracy and reliability of microwave and THz measurements, paving the way for their development and commercialisation in Europe. The measurement and calibration methods developed will be used to more effectively design, manufacture and test high-performance security devices, and to ensure that the devices are used safely. They will help the companies to sell their products in a market where the investors have to be convinced of the benefit of the new technologies and that relies on public acceptance, e.g. of persons to be scanned. By providing reliable measurement data of exposition levels and reliable input for further studies of possible adverse health effects, a majority of users can presumably be convinced to accept the new products.

Microwave and THz radiation can now be harnessed to deliver a new level in non-invasive scanning and detection, with faster and more comfortable security checks.

Environment and social/quality of life impact:

Security checks at airports affect 2.5 billion passengers worldwide per year (source: IATA). A continuously increasing number of these are checked in personnel scanners. In order to protect both operating employees and scanned persons, it is necessary to reliably monitor the conformity of new microwave and THz technologies with the existing safety limits that protect the population from adverse thermal effects of electromagnetic radiation up to 300 GHz and to provide data for further regulatory action regarding the extension of the frequency range of safety limits up to several THz, together with the consideration of possible non-thermal effects, as needed in the future. Also safety standards for laser radiation will benefit from better measurement data. The average electromagnetic radiation intensity is steadily increasing. Electromagnetic radiation has been discussed as a potential enhancing factor for the development of cancer in the population. It is therefore very important to work towards a decrease in the radiation level which could be realised by a factor of 100 if new approaches like software focusing will be implemented in body scanners. This project helped to develop systems with optimum performance (e.g., with steerability of sources and software focusing) at lowest possible radiation levels. Furthermore, it provided reliable dosimetric data for further studies on possible adverse health effects of millimetre and terahertz radiation below the thermal damage level.

The successful implementation of the project helped to establish new scanning technologies in security relevant locations by improving the acceptance of new technologies. In addition to ethical concerns, health concerns had to be addressed to establish millimeter and THz technology successfully. The use of these new security technologies facilitates procedures during security checks (making them easier and more comfortable) while further improving the security. People are able to maintain a mobile and public life style despite increased security threads.

Impact on Standards

This project is among the first standardisation activities performed for scanners and spectrometers in the microwave to THz region. Results may contribute to two overarching standards, IEC/EN 62479 and IEC/EN 62311, which govern the protection of people exposed to electromagnetic fields when using novel devices for which product standards have not yet been established. These standards are a prerequisite for new hardware development, and are essential for securing the public acceptance of new technologies that use electromagnetic radiation. The techniques developed during this project will also be used to demonstrate compliance with European Directive 2004/40/EC "Physical Agents Directive", which sets exposure limits for personnel working with high-frequency radiation, as well as for other applicable national and international guidelines, such as that of the International Commission on Non-Ionising Radiation Protection (ICNIRP). The PTB service has been used to perform a pilot comparison of THz detector calibration capabilities from Germany, China and the USA, an important first step in harmonising international standards.

The project established links to national regulation authorities in Germany (Federal Office for Radiation Protection) and the Czech Republic (National Institute of Public Health) that are concerned with radiation protection of non-ionising radiation and that will take the necessary regulatory steps if needed.

The project also established links to the following standardisation projects and activities:

- IEEE 802.15 Terahertz Interest Group. This group explores the feasibility of the THz band for wireless communication and gives input to the on-going discussion on spectrum allocation beyond 275 GHz at the World Radiocommunication Conference (WRC). The latter is of utmost importance for the future use of spectral resources in security applications. Technical University Braunschweig also collaborated with the project. In July 2013 the Terahertz Interest Group has been upgraded to the study group 100G with the scope of determining the validity of a standard on 100 Gbit/s point-to-point communications. In March 2014 this led to the establishment of the task group 3d (TG3d), which works on an amendment of the 802.15.3 standard targeting 100 Gbit/s for switched point-to-point links.

- DKE/UK 767.4 "Devices and Techniques for Measurement of Electromagnetic Emission" which serves a mirror committee for CLC/TC 210 (EMC) and IEC/CISPR/SC A (Radio interference measurements and statistical methods). The project Coordinator T. Kleine-Ostmann from PTB is member in DKE/UK 767.4.

- The new standardisation project VDI/VDE-GMA FA 8.17 Terahertz Systems which aims at standardisation for industrial applications of THz systems e.g. as sensors or for measurement and imaging tasks has been founded during the project lifetime and profited from input from the project, already.

The establishment of additional links, e.g., to the European Telecommunications Standards Institute (ETSI), was actively pursued. Such links were used to disseminate the scientific results and to actively incorporate the project findings into standardisation in the area of emission measurements in the millimeter and sub-millimeter wave range. This effort ensured a worldwide visibility of the project.

The performed studies give input for the further development of generic standards that regulate the requirements for electromagnetic installations and devices with regard to the protection of humans in electromagnetic fields where no current product standard exists. It supports initiatives for certification and standardisation such as the recently founded coordination site for the security industry (KoSi) within the German Institute for Standardisation (Deutsches Institut für Normung – DIN) helping to develop first product standards for scanner technology.

Dissemination of results

To ensure the uptake of the project's achievements, results have been shared with scientific and industrial end-users through a dedicated website, regular newsletters, the publication of 34 papers in international journals and conference proceedings (listed in the next section), 2 trade journal articles, and 70 conference contributions, including plenary talks during the International Conference on Infrared, Millimeter, and THz Waves, and the Conference on Precision Electromagnetic Measurements.

A training workshop "Security Scanners – Adequate Methods to Measure the Exposure" was held at Rohde & Schwarz GmbH & Co. KG in Munich, with participants from industry, research organisations and authorities.

A best practice guide based on the workshop results is available on the project webpage and EURAMET repository, and enables producers, users and regulators to reliably measure the performance of THz security scanners.

Results were presented at the final project workshop to stakeholders in industry, universities and regulatory authorities, focusing on the detector technology and calibration, and the use and validation of THz spectrometers.

5   Website address and contact details

Project website:

http://www.ptb.de/emrp/804.html

Project coordinator:

Dr. Thomas Kleine-Ostmann
Physikalisch-Technische Bundesanstalt (PTB)
2.21 Electromagnetic Fields and Antenna Measuring Techniques
Bundesallee 100, D-38116 Braunschweig
Germany
phone: +49-531-592-2210
fax: +49-531-592-69-2256
email: thomas.kleine-ostmann@ptb.de

6   List of publications

Kazemipour, S.-K. Yee, M. Hudlicka, M. Salhi, T. Kleine-Ostmann, T. Schrader, Design and Calibration of a Compact Quasi-Optical System for Material Characterisation in Millimeter/Sub-millimeter Wave Domain, Conference on Precision Electromagnetic Measurements 2014, Rio de Janeiro, Brazil, pp. 482-483, DOI: 10.1109/CPEM.2014.6898469

A. Kazemipour, M. Hudlicka, T. Kleine-Ostmann, T. Schrader, A Reliable Simple Method to Extract the Intrinsic Material Properties in Millimeter/Sub-millimeter Wave Domain, Conference on Precision Electromagnetic Measurements 2014, Rio de Janeiro, Brazil, pp. 576-577, DOI: 10.1109/CPEM.2014.6898516

A. Kazemipour, M. Hudlicka, R. Dickhoff, M. Salhi, T. Kleine-Ostmann, T. Schrader, The Horn Antenna as Gaussian-Source in the mm-Wave Domain, Journal of Infrared, Millimeter, and Terahertz Waves, 2014, Vol. 35, No. 9, pp. 720-731, DOI: 10.1007/s10762-014-0077-9

A. Kazemipour, M. Hudlicka, S.-K. Yee, M. Salhi, D. Allal, T. Kleine-Ostmann, T. Schrader, Design and Calibration of a Compact Quasi-Optical System for Material Characterisation in Millimeter/Submillimeter Wave Domain, IEEE Transactions on Instrumentation and Measurement, 2015, Vol. 64, pp. 1438-1445, DOI: 10.1109/TIM.2014.2376115

A. Kazemipour, M. Hudlicka, S.-K. Yee, M. Salhi, T. Kleine-Ostmann, T. Schrader, Wideband Frequency-Domain Material Characterisation Up To 500 GHz, 39th International Conference on Infrared, Millimeter, and THz Waves, The University of Arizona, Tucson, AZ, page P1-30 M5-P7.12, DOI: 10.1109/IRMMW-THz.2014.6956130

A. Kazemipour, M. Salhi, M. Hudlicka, T. Kleine-Ostmann, T. Schrader, Probe Correction For Near-Field Scanning With A Dielectric Fiber, 39th International Conference on Infrared, Millimeter, and THz Waves, The University of Arizona, Tucson, AZ, page T2/B-17.5, DOI: 10.1109/IRMMW-THz.2014.6956288

A. Kazemipour, M. Hudlicka, M. Salhi, T. Kleine-Ostmann, T. Schrader, Free-space Quasi-optical Spectrometer for Material Characterisation in the 50-500 GHz Frequency Range, 44th European Microwave Conference, Rome, Italy, October 06-09, 2014, pp.636 - 639, DOI: 10.1109/EuMC.2014.6986514

Y. Deng, H. Füser, and M. Bieler, Absolute intensity measurements of cw GHz and THz radiation using electro-optic sampling, IEEE Transactions on Instrumentation and Measurement, 2015, Vol. 64, pp. 1734 - 1740, DOI: 10.1109/TIM.2014.2375692

Chromik, Š., Štrbik, V., Dobročka, E., Roch, T., Rosová, A., Španková, M., Lalinský, T., Vanko, G., Lobotka, P., Ralbovský, M., Choleva, P., LSMO thin films with high metal-insulator transition temperature on buffered SOI substrates for uncooled microbolometers, Applied Surface Science, 312 (2014) 30-33.

Štrbik, V., Reiffers, M., Dobročka, E., Šoltýs, J., Španková, M., Chromik, Š., Epitaxial LSMO thin films with correlation of electrical and magnetic properties above 400K, Applied Surface Science, 312 (2014) 212-215.

L. Oberto, M. Bisi, D. Jahn, S. Lippert, L. Brunetti, Set-up of a THz Time Domain Spectrometer at INRIM, Conference on Precision Electromagnetic Measurements 2014, Rio de Janeiro, Brazil, pp. 188-189, DOI: 10.1109/CPEM.2014.6898322

A. Kazemipour, M. Salhi, T. Kleine-Ostmann, T. Schrader, A Simple New Method to Calibrate Millimeter-Wave Mixers, IEEE Design & Test, 31, 46-51 (2014), DOI:10.1109/MDAT.2014.2355419

Andreas Steiger, Mathias Kehrt, Christian Monte, and Ralf Müller, Traceable terahertz power measurement from 1 THz to 5 THz, Optics Express, Jun 2013, Vol. 21, Issue 12, pp. 14466-14473

Ralf Müller, Werner Bohmeyer, Mathias Kehrt, Karsten Lange, Christian Monte, and Andreas Steiger, Novel detectors for traceable THz power measurements, J Infrared Milli Terahz Waves 35 (2014) 659–670 DOI: 10.1007s10762-014-0066-z

Heiko Füser and Mark Bieler, Terahertz Frequency Combs, Journal of Infrared, Millimeter, and Terahertz Waves, 2014, Vol. 35, pp 585-609 , DOI: 10.1007/s10762-013-0038-8

L. Zilberti, A. Arduino, O. Bottauscio, M. Chiampi, Parametric Analysis of Transient Skin Heating Induced by Terahertz Radiation, Bioelectromagnetics, Vol. 35, n. 5, July 2014, pp. 314-323.

Chromik, Š., Štrbik, V., Dobročka, E., Laurenčíková, A., Reiffers, M., Liday, J., Španková, M., Significant increasing of onset temperature of FM transition in LSMO thin films, Applied Surface Science, 269 (2013) 98-101.

Štrbík, V., Reiffers, M., Chromik, Š., Španková, M., Approximation of electrical and magneto transport properties of LSMO thin films, Acta Phys. Polonica A, 26 (2014) 210-211.

Španková, M., Chromik, Š., Dobročka, E., Štrbik, V., Sojková, M, LSMO films with increased temperature of MI transition, Acta Phys. Polonica A, 126 (2014) 212-213.

Luca Zilberti, Damien Voyer, Oriano Bottauscio, Mario Chiampi, Riccardo Scorretti, Effect of tissue parameters on skin heating due to millimeter EM waves, IEEE Transactions on Magnetics, 2015, Vol. 51, 9400904, DOI: 10.1109/TMAG.2014.2363898

Oriano Bottauscio, Mario Chiampi and Luca Zilberti, Thermal Analysis of Human Tissues Exposed to Focused Beam THz Radiations, IEEE Transactions on Magnetics, 2015, Vol. 51, 7400504, DOI: 10.1109/TMAG.2014.2355260

M. Charles and D. Allal, Metrological Measurements in Terahertz Time-Domain Spectroscopy at LNE (From 100 GHz to 2 THz), Conference on Precision Electromagnetic Measurements 2014, Rio de Janeiro, Brazil, pp. 180-181

A. Steiger, R. Müller, High Precision THz Radiometry, 38th International Conference on Infrared, Millimeter, and THz Waves, Mainz, Germany, Sept. 2013, DOI: 10.1109/IRMMW-THz.2013.6665713

R. Müller, W. Bohmeyer, M. Kehrt, K. Lange, C. Monte, and A. Steiger, Novel Broadband THz-Detector, 38th International Conference on Infrared, Millimeter, and THz Waves, Mainz, Germany, Sept. 2013, DOI: 10.1109/IRMMW-THz.2013.6665749

T. Kleine-Ostmann, THz Metrology, 38th International Conference on Infrared, Millimeter, and THz Waves, Mainz, Germany, Sept. 2013, DOI: 10.1109/IRMMW-THz.2013.6665913

S. Augustin, R. Bretfeld, U. Böttger, H. Hirsch, H. Richter, A. Semenov and H.-W. Hübers, Passive stand-off THz imaging using lock-in phase information, 38th International Conference on Infrared, Millimeter, and THz Waves, Mainz, Germany, Sept. 2013, DOI: 10.1109/IRMMW-THz.2013.6665770

A. Kazemipour, M. Salhi, T. Kleine-Ostmann and T. Schrader, Novel Method to Measure the Conversion-Losses (C.L.) of Microwave and mm-Wave Mixers, Asia-Pacific Microwave Conference 2013, Seoul, Korea, Nov. 2013, pp. 731 - 733, DOI: 10.1109/APMC.2013.6694912

A. Kazemipour, T. Kleine-Ostmann and T. Schrader, Analytical Study of mm-Wave and THz Beams, Application to RF-Metrology, Asia-Pacific Microwave Conference 2013, Seoul, Korea, Nov. 2013, pp. 1206 - 1208, DOI: 10.1109/APMC.2013.6695072

Ralf Müller, Berndt Gutschwager, Jörg Hollandt, Mathias Kehrt, Christian Monte, Ralph Müller, and Andreas Steiger, Characterisation of a large-area pyroelectric detector from 300 GHz to 30 THz, J Infrared Milli Terahz Waves 36 (2015) 654–661, DOI 10.1007/s10762-015-0163-7

Alireza Kazemipour, Thomas Kleine-Ostmann, Thorsten Schrader, Djamel Allal, Michael Charles, Luca Zilberti, Michele Borsero, Oriano Bottauscio, Mario Chiampi, Assessing the heat transfer into the human skin after exposure to mm and sub-mm waves, submitted to Microwave Journal.

Ralf Müller, Andreas Steiger, Karsten Lange, Werner Bohmeyer, Calibrated Measurement of THz Radiation, submitted to Photonik.